

FACULTY OF MATHEMATICS,
PHYSICS AND INFORMATICS
Comenius University
Bratislava



Simulation of the propagation of ultra-high energy cosmic rays using SimProp software

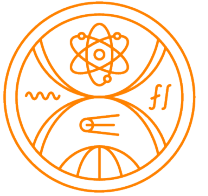
Mgr. Patrik Čechvala
patrik.cechvala@fmph.uniba.sk

doktorand

Ing. Jakub Vícha, PhD., FZÚ ČAV



Content



- Main characteristics of ultra-high energy cosmic rays (UHECRs) – energy spectrum, mass composition, propagation processes
- Simulation code *SimProp*
- Results of our work – evolution of $\langle \ln A_{\text{Earth}} \rangle$ and selection of simulations compatible with the shape of the energy spectrum measured by the Pierre Auger Observatory
- Summary



UHECRs and their main properties

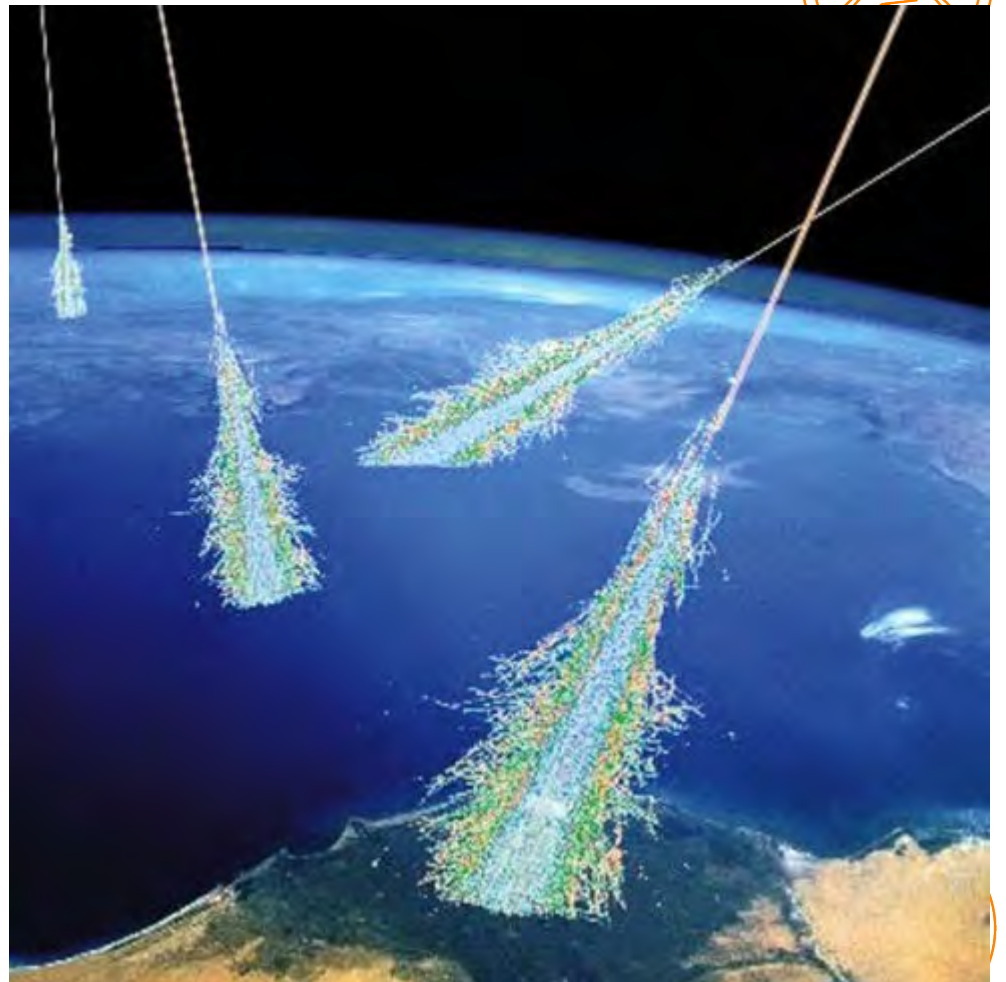


Cosmic rays (CRs)

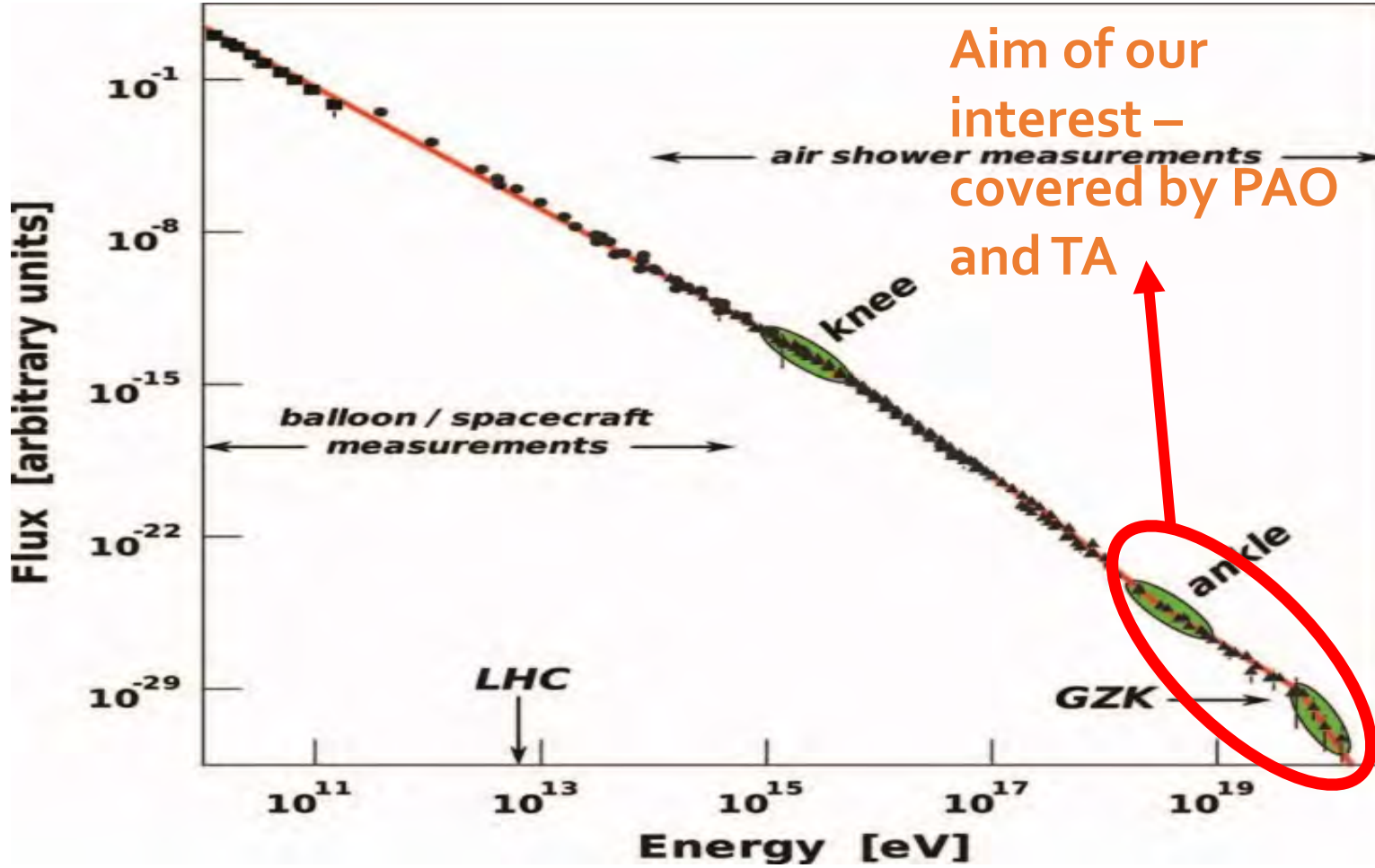


- Particles propagating through the Universe colliding with the Earth's atmosphere – mainly protons and nuclei of different elements
- Particles with sufficient energy ($> 100 \text{ TeV}$) generate showers of secondary particles in the atmosphere
- Observations by arrays of surface detectors and fluorescence detectors
- At energies $> 10^{18} \text{ eV}$ – the Pierre Auger Observatory (PAO) and Telescope Array (TA)

Source:
<https://www.auger.org/index.php/cosmic-rays/cosmic-ray-mystery>



Energy spectrum



(Zavrtanik, 2010)

Energy spectrum

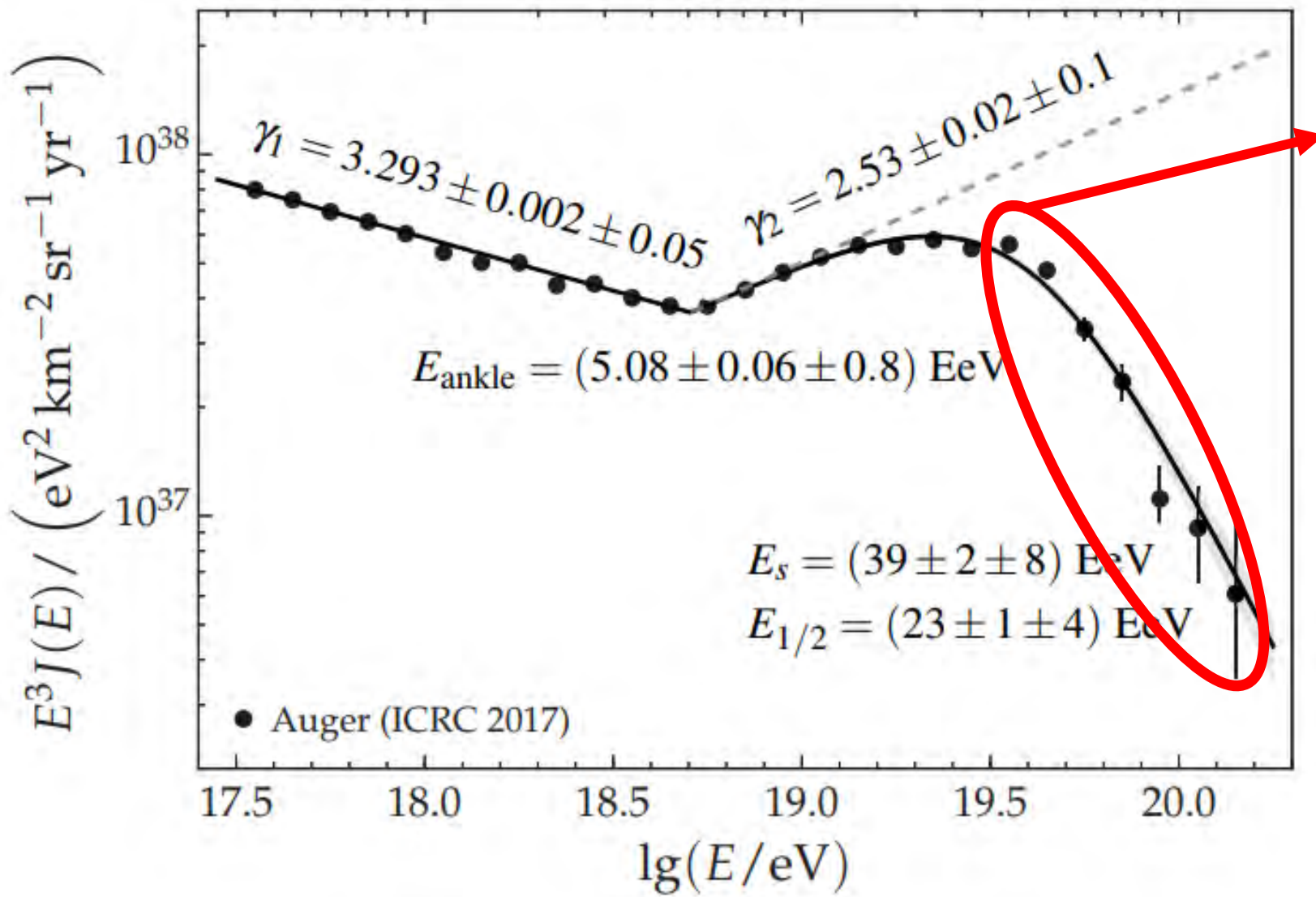


- Approximation by a simple power-law

$$J(E) \approx E^{-\gamma}$$

- γ – spectral index
- Regions where the spectral index changes
 - „knee“ – steepening at $10^{15.6}$ eV (KASCADE Collaboration, 2005)
 - Below knee $\gamma \approx 2.7 \pm 0.01$
 - Above knee $\gamma \approx 3.1 \pm 0.07$
 - „ankle“ – hardening of the spectrum, spectral index decreases at energies $\approx 3 \cdot 10^{18}$ eV
 - suppression at the highest energies $\approx 10^{19.7}$ eV – usually „GZK“ cutoff ($\gamma \approx 4.8$)





(Fenu for the Pierre Auger Collaboration, 2017)

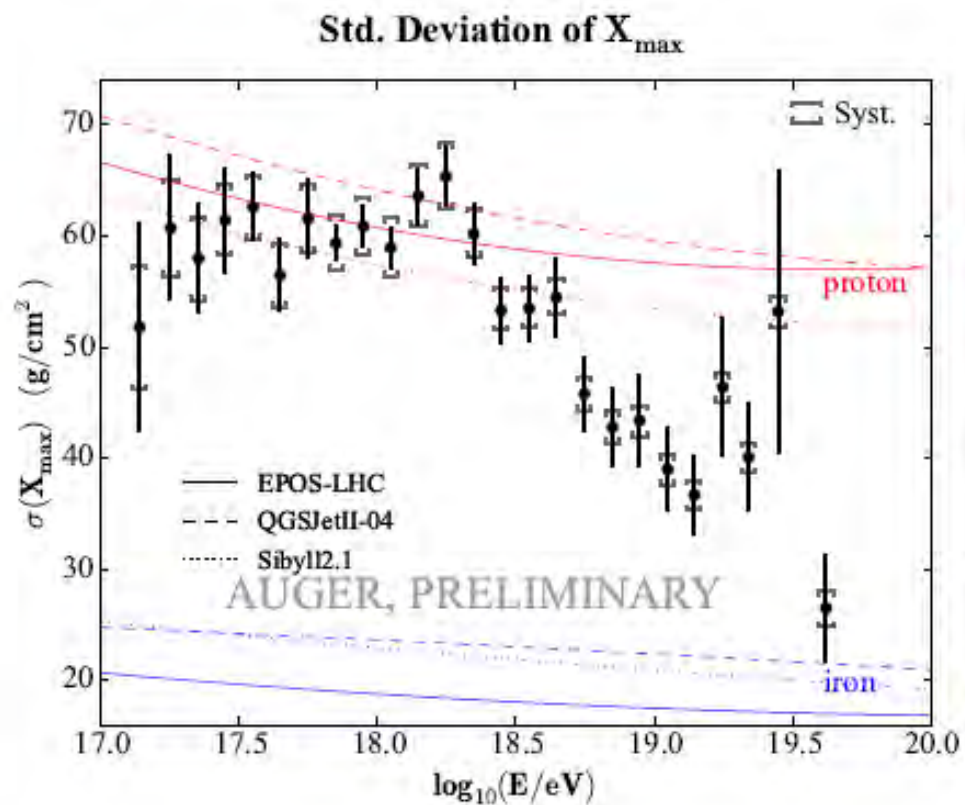
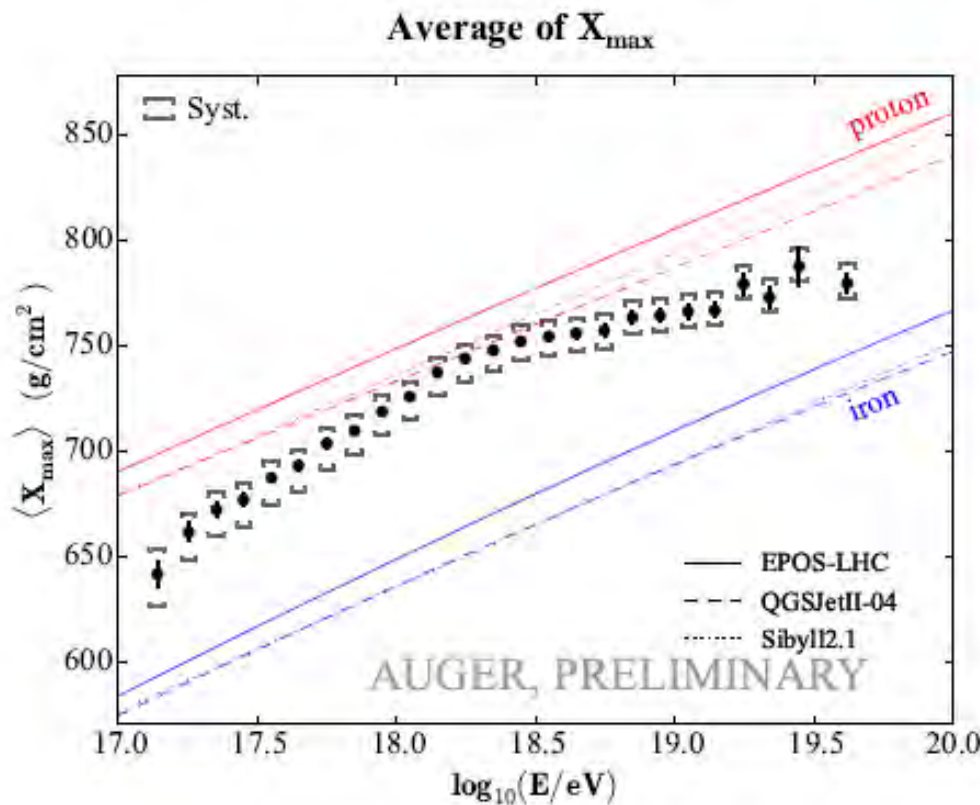


Can be caused by a single source?



Mass composition of UHECRs

- Measurements of X_{\max}





$$X = \int_{\infty}^h \frac{\rho(l)}{\cos \theta} dl$$

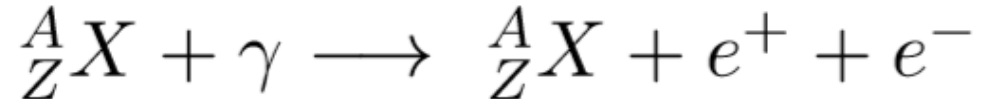
- $\rho(l)$ – the density of air at altitude l
- θ – zenith angle

- PAO measurements
 - up to $10^{18.3}$ eV – composition becomes gradually lighter
 - above $10^{18.3}$ eV – trend inverts, composition is getting heavier



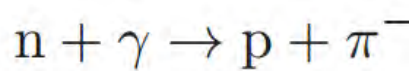
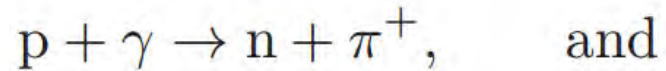
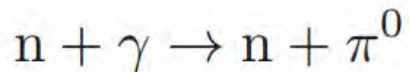
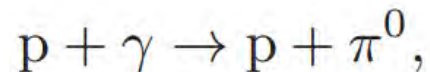
Interaction processes

- Pair production



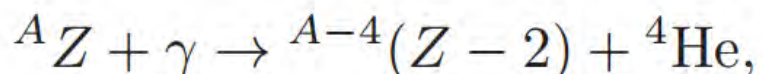
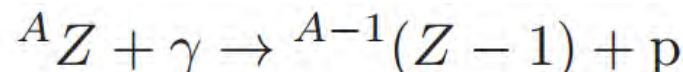
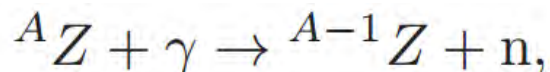
$$E_{\text{thres}}^{e^\pm} = \frac{m_e(m_X + m_e)}{\epsilon} \approx 4.8 \cdot 10^{17} A \left(\frac{\epsilon}{10^{-3} \text{ eV}} \right)^{-1} \text{ eV}$$

- Photo-pion production



$$E_{\text{thres}}^{N,\pi} = \frac{m_\pi(m_N + m_\pi/2)}{2\epsilon} \approx 6.8 \cdot 10^{19} \left(\frac{\epsilon}{10^{-3} \text{ eV}} \right)^{-1} \text{ eV},$$

- Photodisintegration

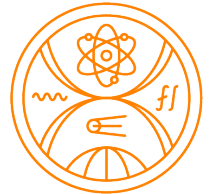


etc.

- Several photodisintegration processes – giant dipole resonance, quasi-deuteron process and baryonic resonance



Other processes



- Adiabatic energy loss due to the expansion of the Universe

$$\left(-\frac{1}{E} \frac{dE}{dt} \right)_{\text{ad}} = H(t) = H_0 \sqrt{(1+z)^3 \Omega_m + \Omega_\Lambda}$$

- Decay of unstable particles
- Interaction with the magnetic fields – trajectories are curved

$$\left(\frac{r_L}{\text{pc}} \right) = 1.1 \left(\frac{E}{\text{PeV}} \right) \left(\frac{\mu\text{G}}{B} \right) \frac{1}{Z}$$

(Kuempel, 2014)

r_L – Larmor radius in pc

B – intensity of magnetic field in μG

E – energy in PeV

Z – charge of the particle



SimProp v2r4



- Monte Carlo code that simulate the propagation of UHECRs
- Written in C++
- Several options
- Output files in ROOT
- All previous processes implemented except of magnetic field deflection



Library of simulations

- Selection of a specific model of background fields – compatible with the reference model of PAO combined fit
 - Gilmore EBL model
 - PSB cross section
 - Decay of unstable particles – enabled
 - Photo-pion production – stochastic on CMB and EBL photons
 - Rigidity cutoff
- Propagation is rectilinear – magnetic fields not incorporated in *SimProp*
- We adopted a single-source scenario of extragalactic CRs at the specific distance and spectral index
- **Number of injected events – 10^5**
- **Injected nuclei – hydrogen ${}^1\text{H}$, helium ${}^4\text{He}$, carbon ${}^{12}\text{C}$, oxygen ${}^{16}\text{O}$, silicon ${}^{28}\text{Si}$ and iron ${}^{56}\text{Fe}$**
- **Distance – 5, 50, 100 Mpc**
- **Injection energy – $\log(E/\text{eV}) = (19.0 - 21.0)$**
- **Spectral index – 1, 1.5, 2, 2.5, 3**
- Library reweighted according to the **rigidity cutoff R_{Cut}**



Theoretically predicted range

$$\gamma_{\text{Source}} = 1.0 - 2.2$$



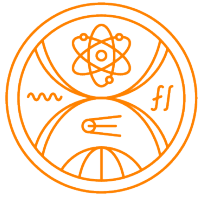
Library of simulations

- Selection of a specific model of background fields – compatible with the reference model of PAO combined fit
 - Gilmore EBL model
 - PSB cross section
 - Decay of unstable particles – enabled
 - Photo-pion production – stochastic on CMB and EBL photons
 - Rigidity cutoff
- Propagation is rectilinear – magnetic fields not included in *SimProp*
- We adopted a single-source scenario
- Number of injected events
- Injected nuclei – hydrogen and iron ^{56}Fe
- Distance – 5, 50, 100 pc
- Injection energy – $\log(E) = 10.5 \pm 0.5$
- Spectral index – 1, 1.5, 2, 2.5
- Library reweighted according to the rigidity cutoff R_{Cut}



These are the parameters of sources that were studied

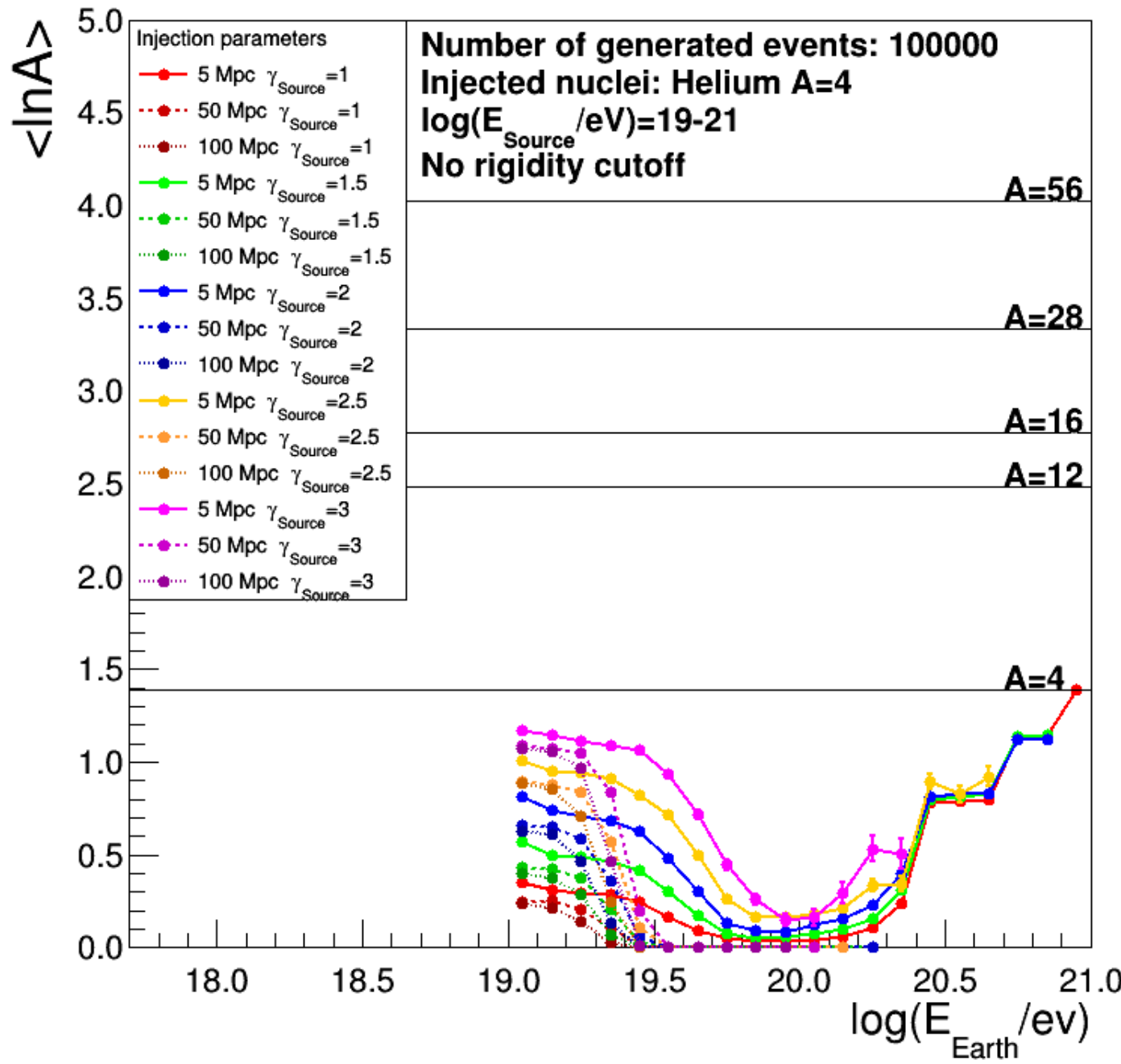




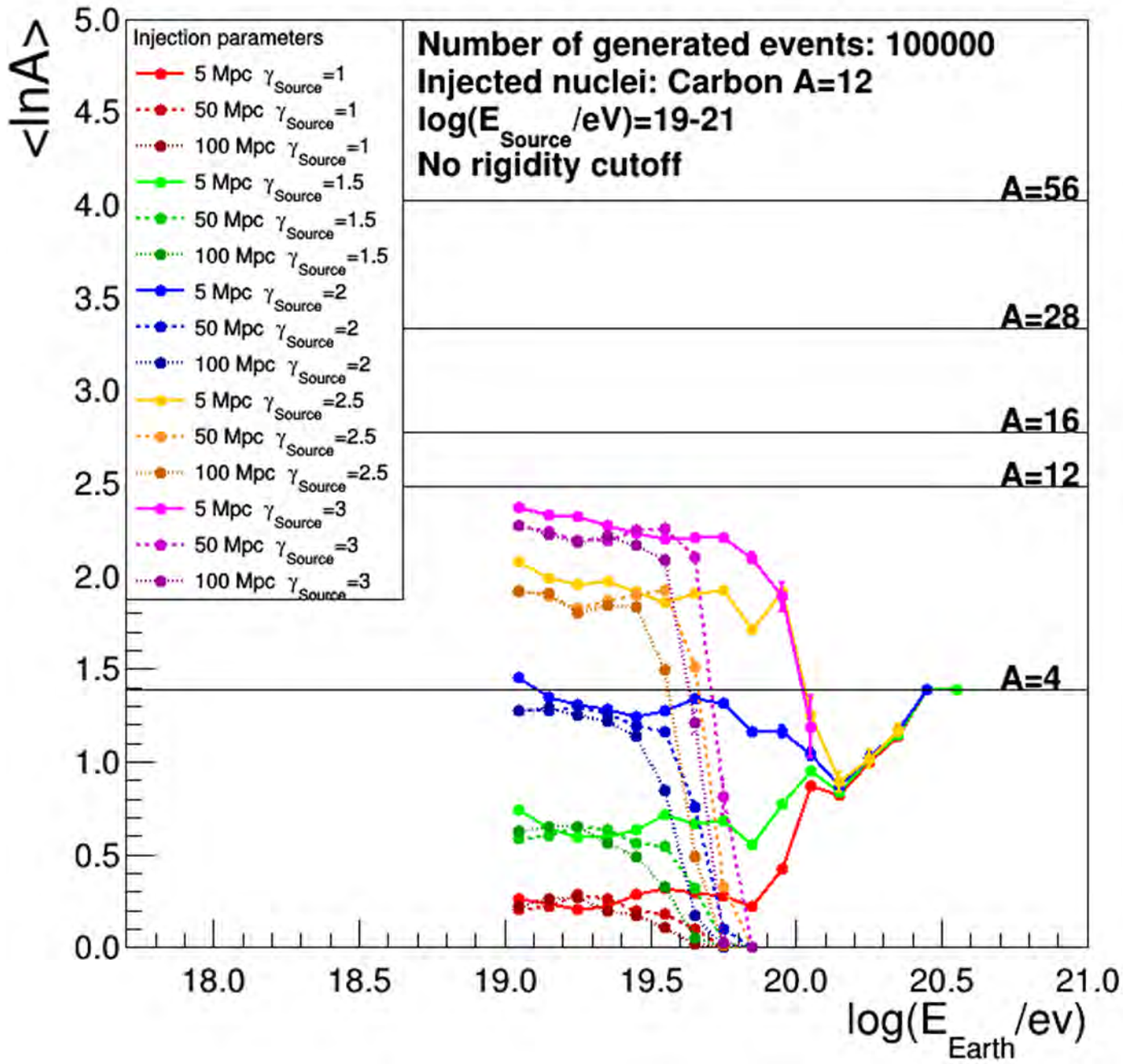
1. Evolution of $\langle \ln A_{\text{Earth}} \rangle$



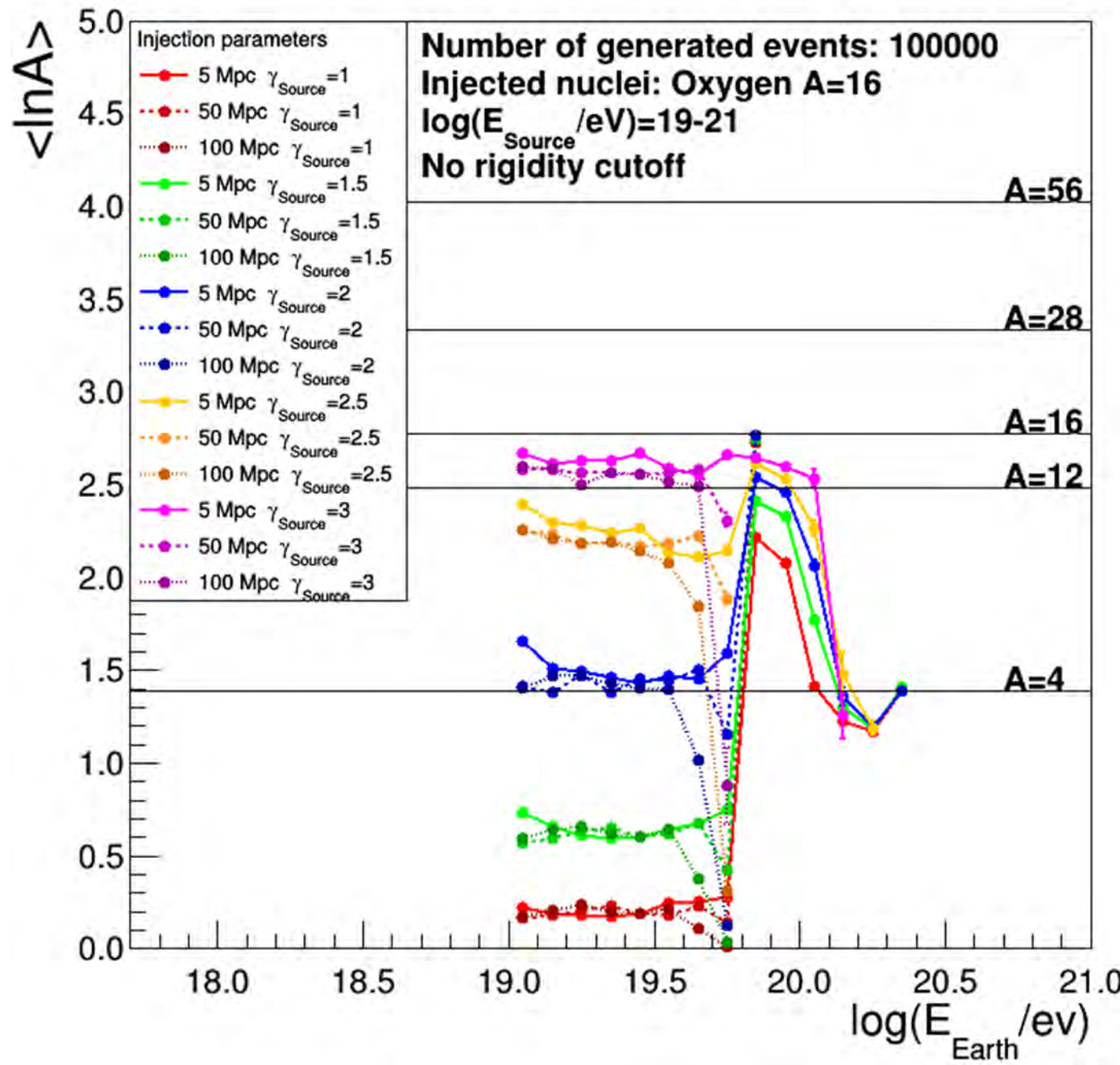
Helium



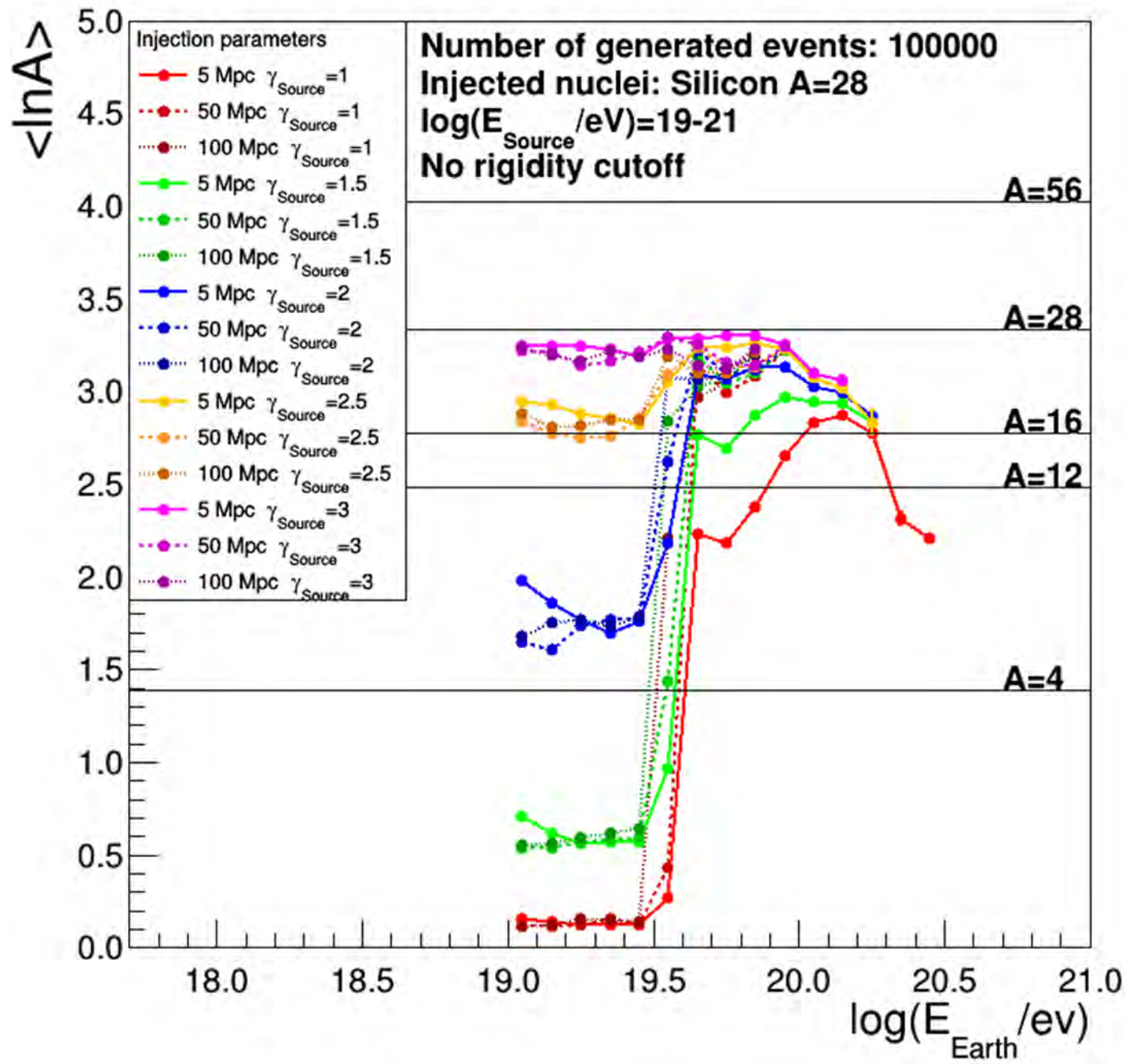
Carbon



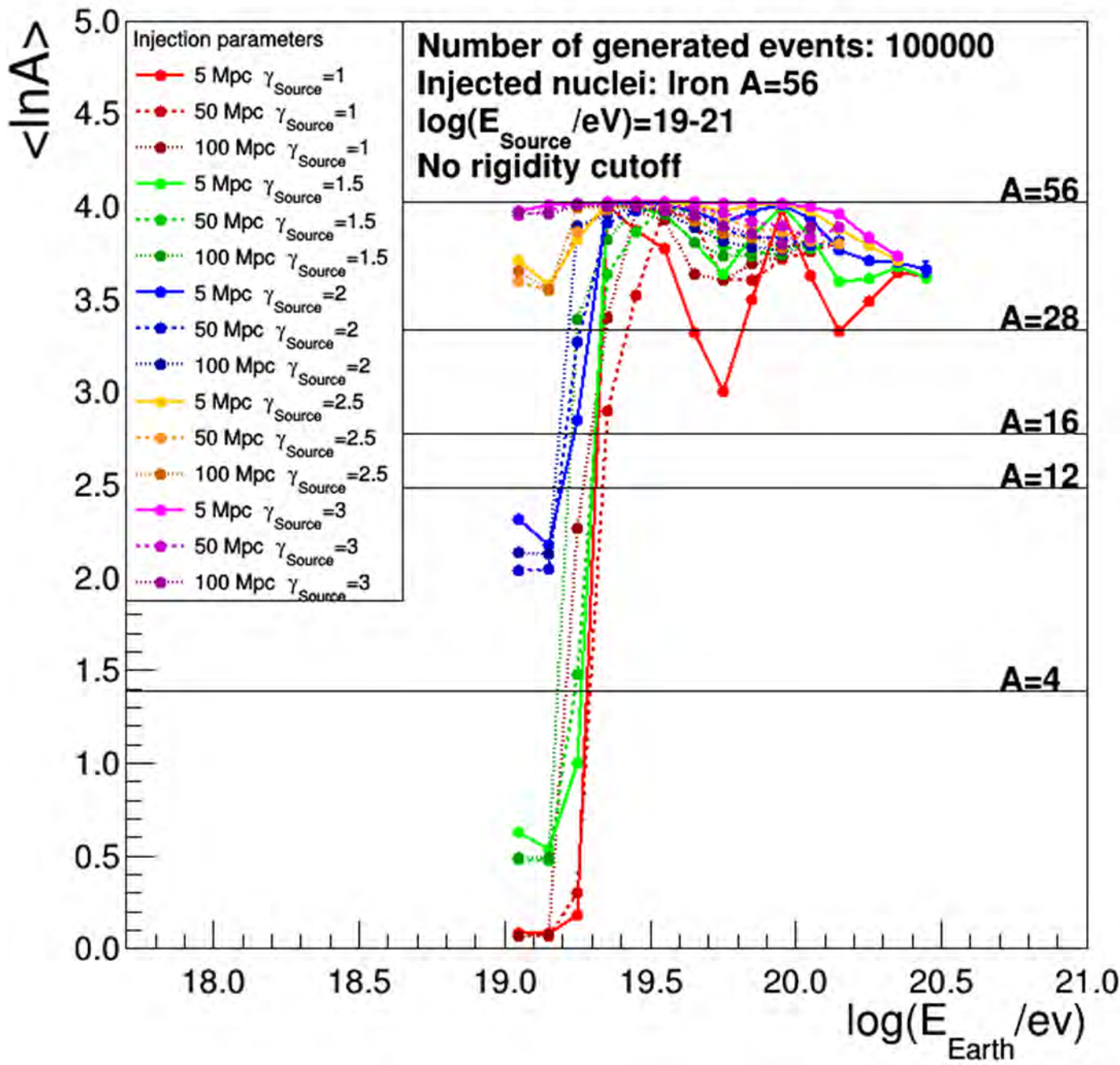
Oxygen

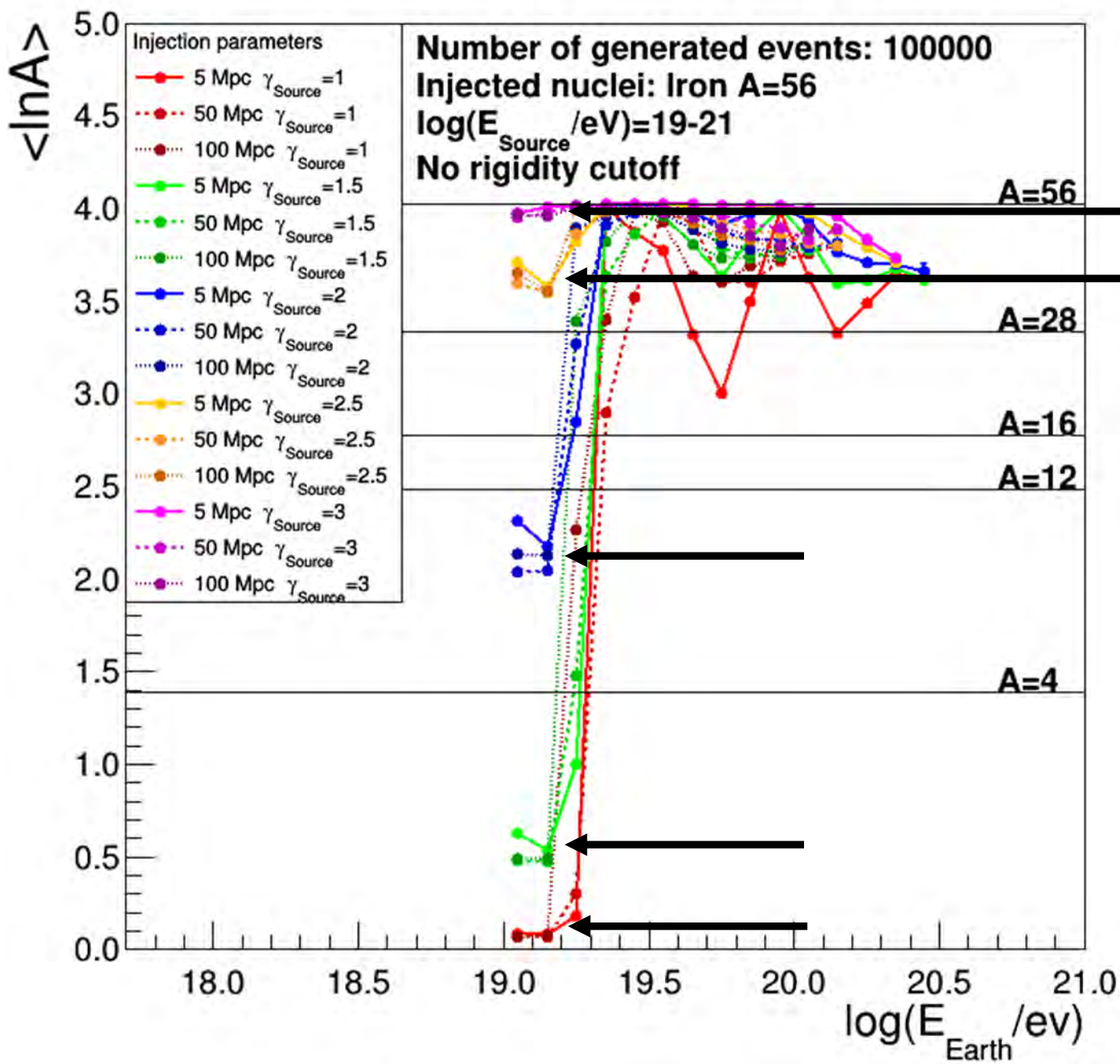


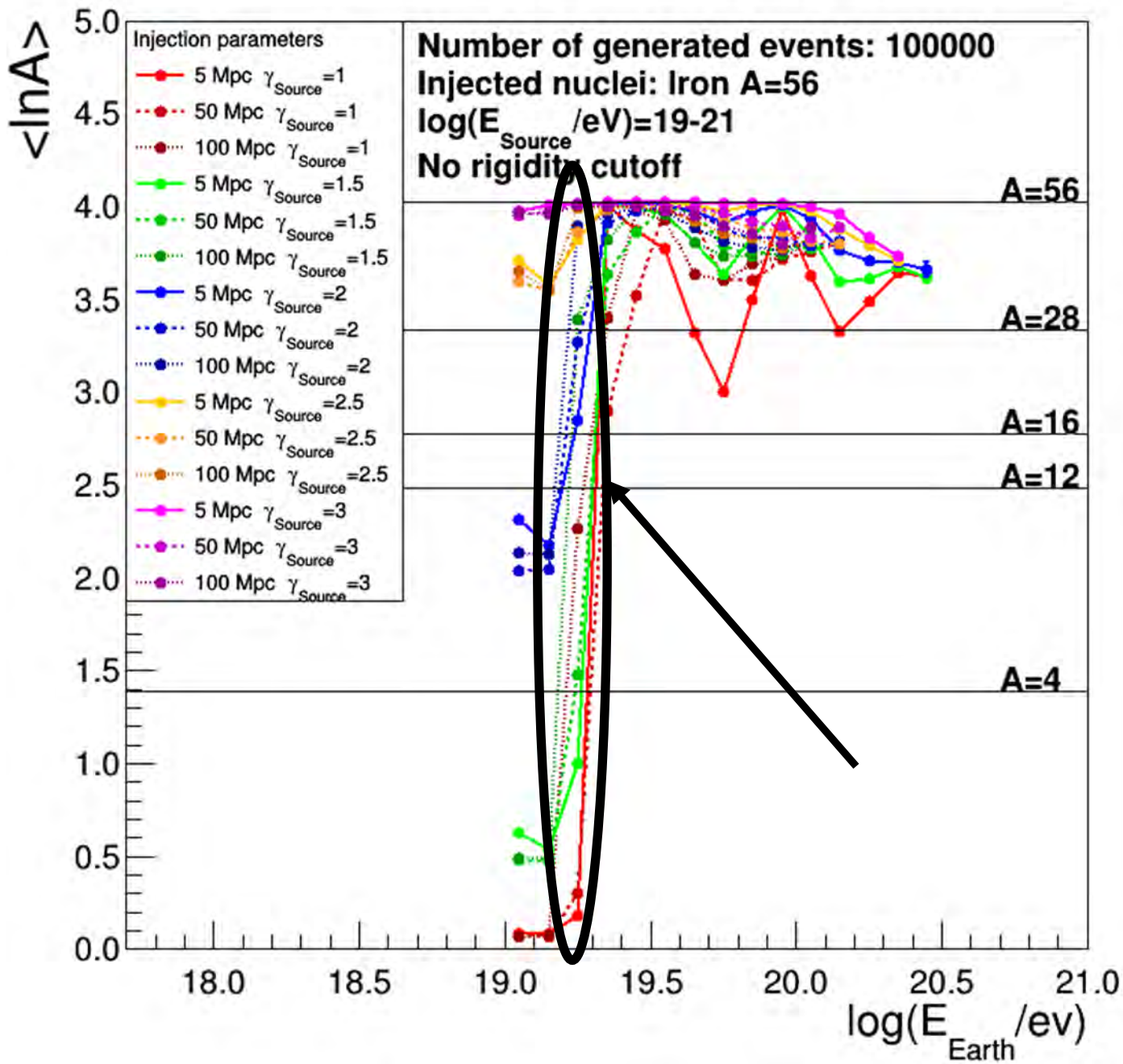
Silicon



Iron









- A sharp increase at different energies for different elements
- Position of the increase

- Oxygen - $E_{Tr}^O \approx 10^{19.75} \text{ eV}$

- Iron - $E_{Tr}^{Fe} \approx 10^{19.15} \text{ eV}$

$$10^{19.75 - 19.15} \approx \frac{56}{16}$$

- Maximum energies of ejected protons depend on the nuclei type and their maximum energies
- However rigidity cutoff can smear the effect

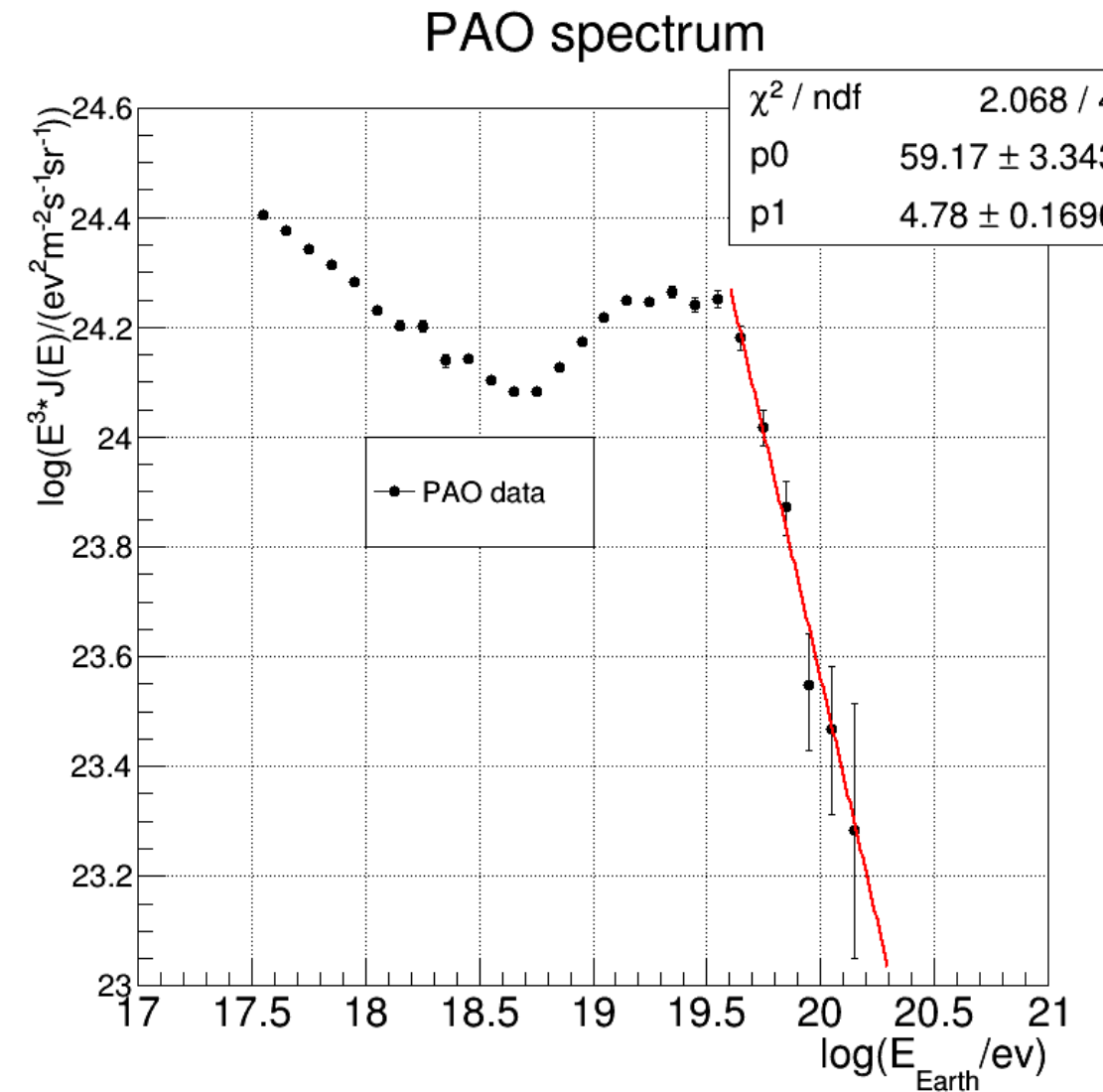


2. Testing compatibility of our simulations with the PAO data



Linear fit

$$y = p_0 - (p_1 - 3) \times \log(E_{\text{Earth}}/\text{eV})$$

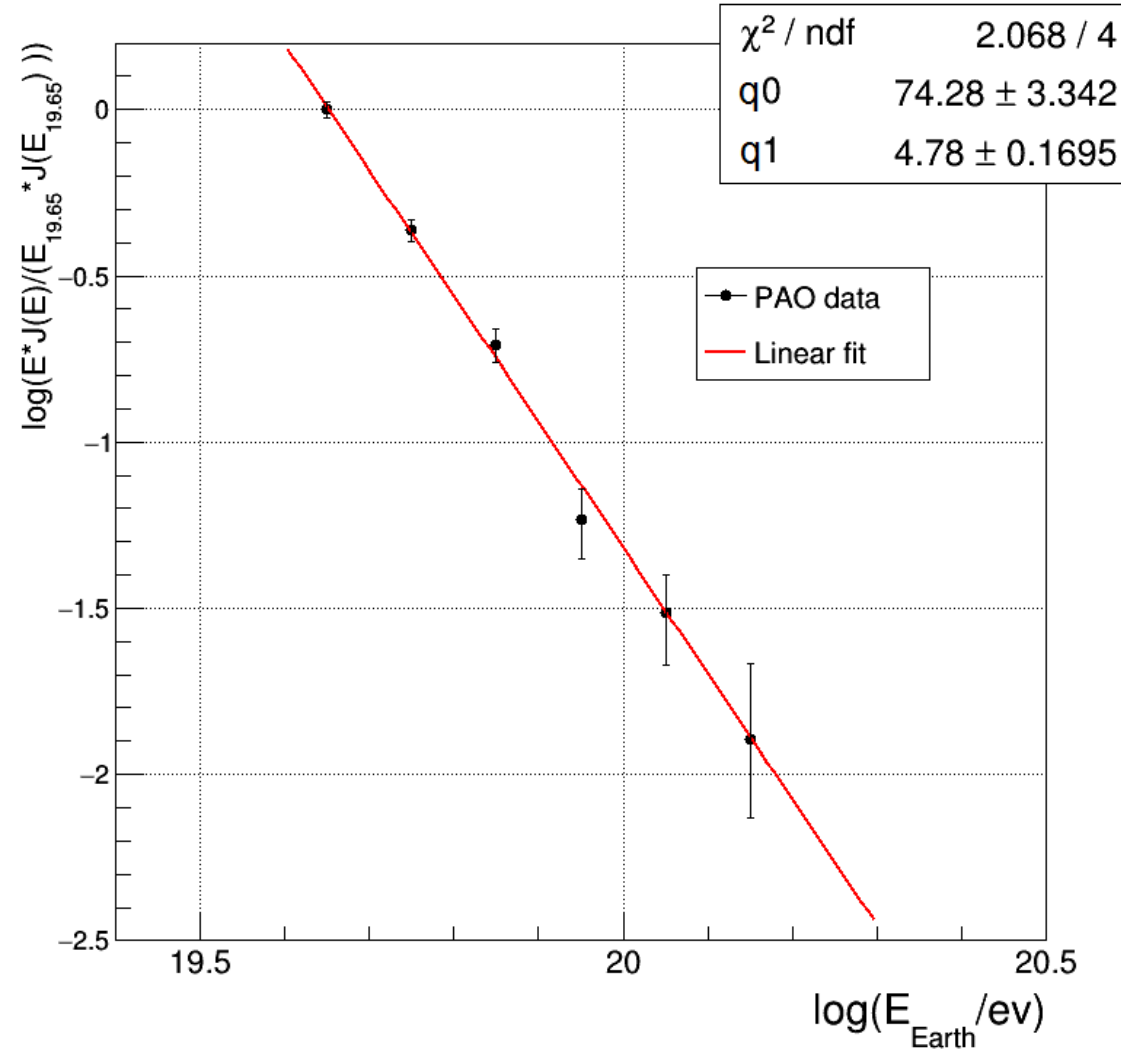


2. Testing compatibility of our simulations with the PAO data



- Normalization of PAO data to the value at energy $\log(E_{\text{Earth}}/\text{eV}) = 19.65$

Normalized PAO spectrum



Linear fit

$$y = q_0 - (q_1 - 1) \times \log(E_{\text{Earth}}/\text{eV})$$

Only the shape of the energy spectrum is what matters in the following analysis



2. Testing compatibility of our simulations with the PAO data



- Nuclei considered – hydrogen ${}^1\text{H}$, helium ${}^4\text{He}$, oxygen ${}^{16}\text{O}$ and iron ${}^{56}\text{Fe}$
- Cutoff rigidity $\log(R_{\text{Cut}}/V) = (19.0 - 21.0)$ incremented by $\Delta \log(R_{\text{Cut}}/V) = 0.1$
- Mixed composition – combinations of different nuclei, equal fractions
 - „H“ or „He“ – pure composition
 - „H+He“ – 50% of hydrogen and 50% of helium
- In total 4 free parameters – R_{Cut} , γ_{Source} , D_{source} , $\langle \ln A_{\text{Source}} \rangle$
- This represents 4725 different combinations





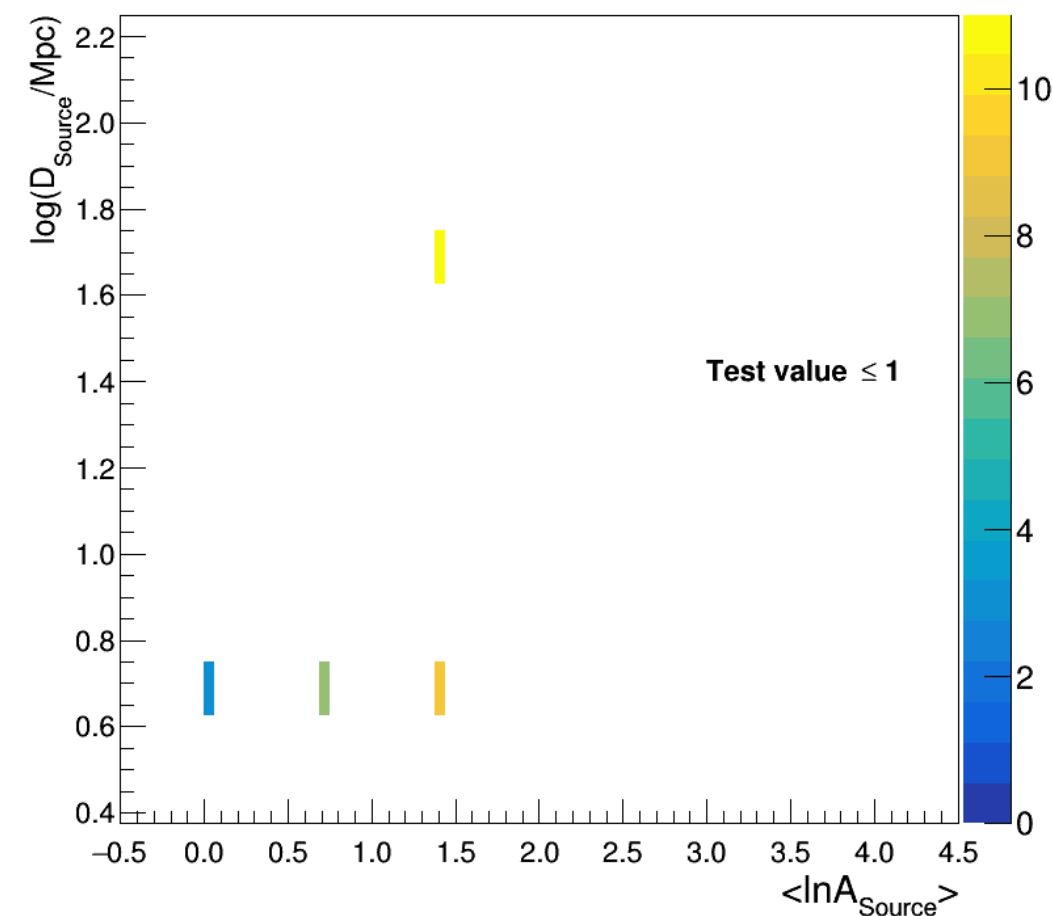
- Dispersion between the PAO datapoints and simulation datapoints represented by „Test value“

$$Test\ value = \frac{1}{n} \sum_{i=1}^n \frac{|N_{P,i} - N_{S,i}|}{\sqrt{\sigma_{P,i}^2 + \sigma_{S,i}^2}}$$

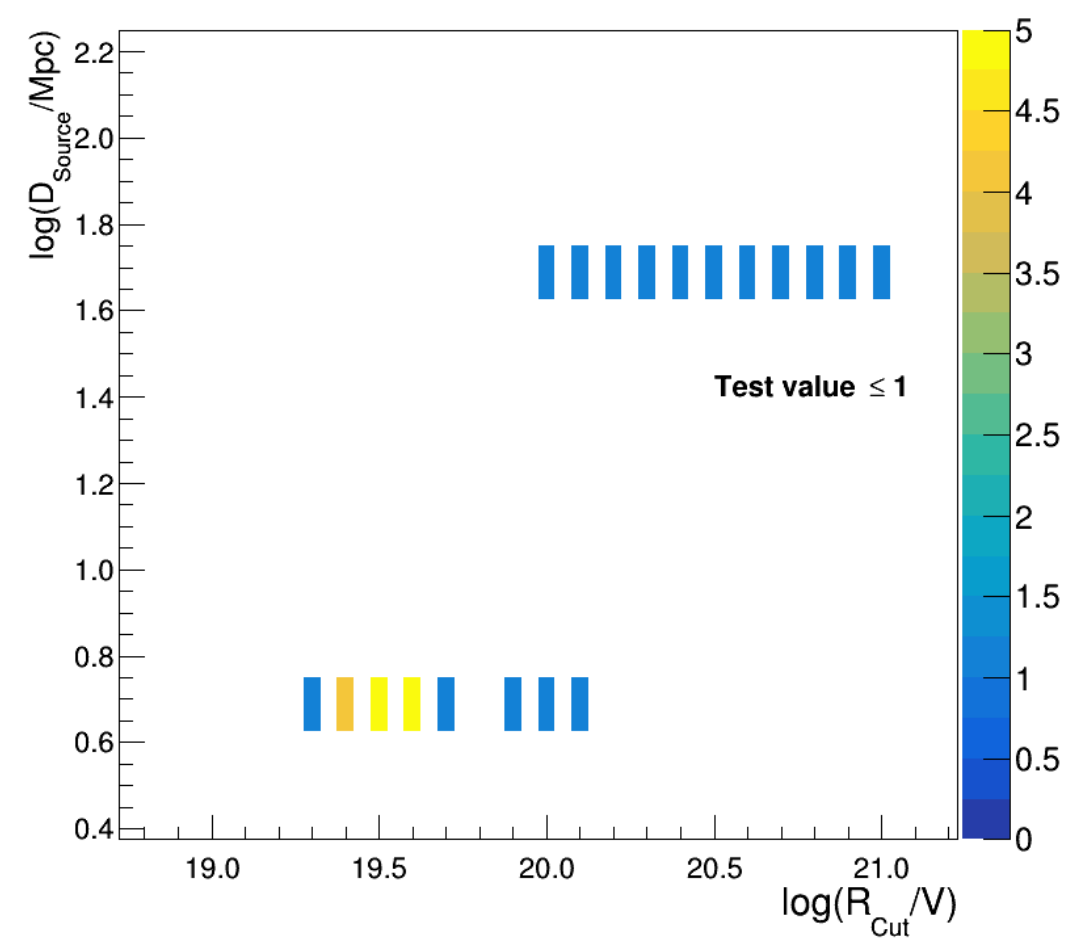
- where $N_{P,i}$ and $N_{S,i}$ are the values of PAO datapoint and simulated datapoint
- $\sigma_{N,i}$ and $\sigma_{S,i}$ are their uncertainties
- Simulation with **Test value ≤ 1 accepted** – 30 simulations satisfy this condition



Distance vs composition at source

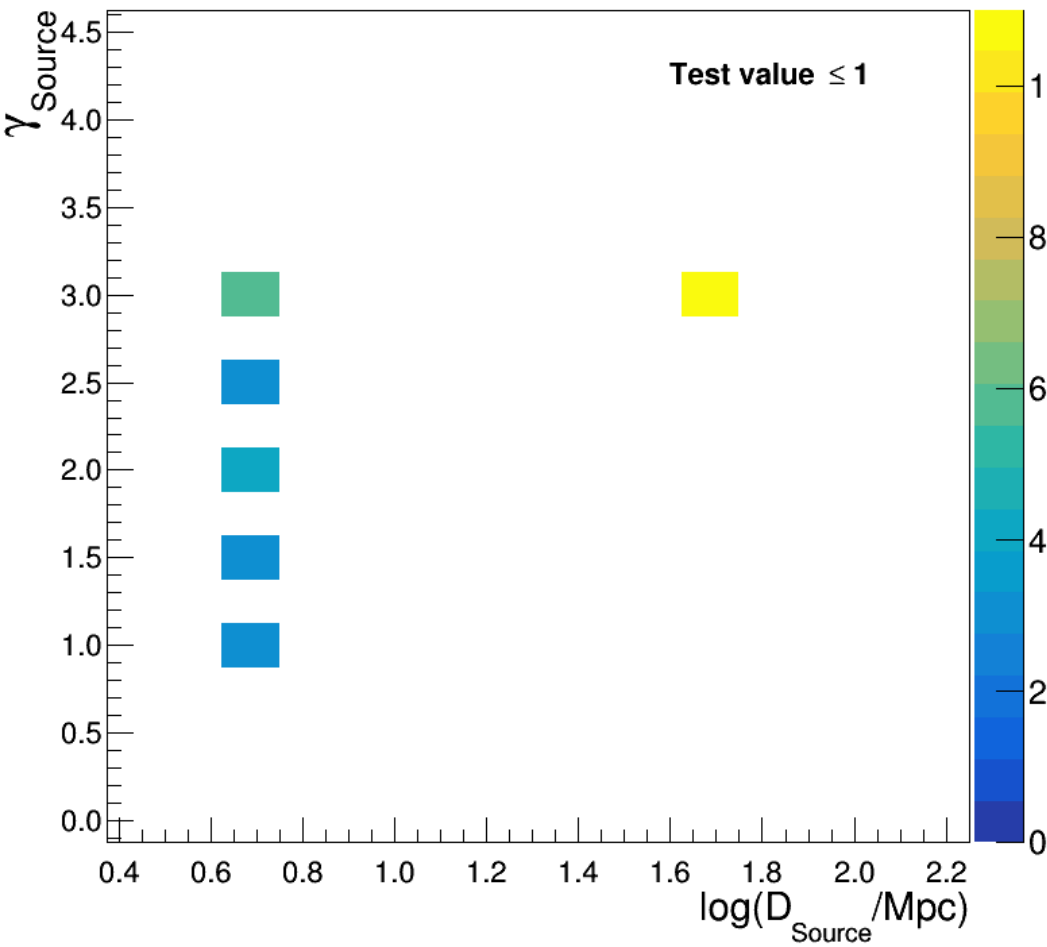


Distance vs cutoff rigidity

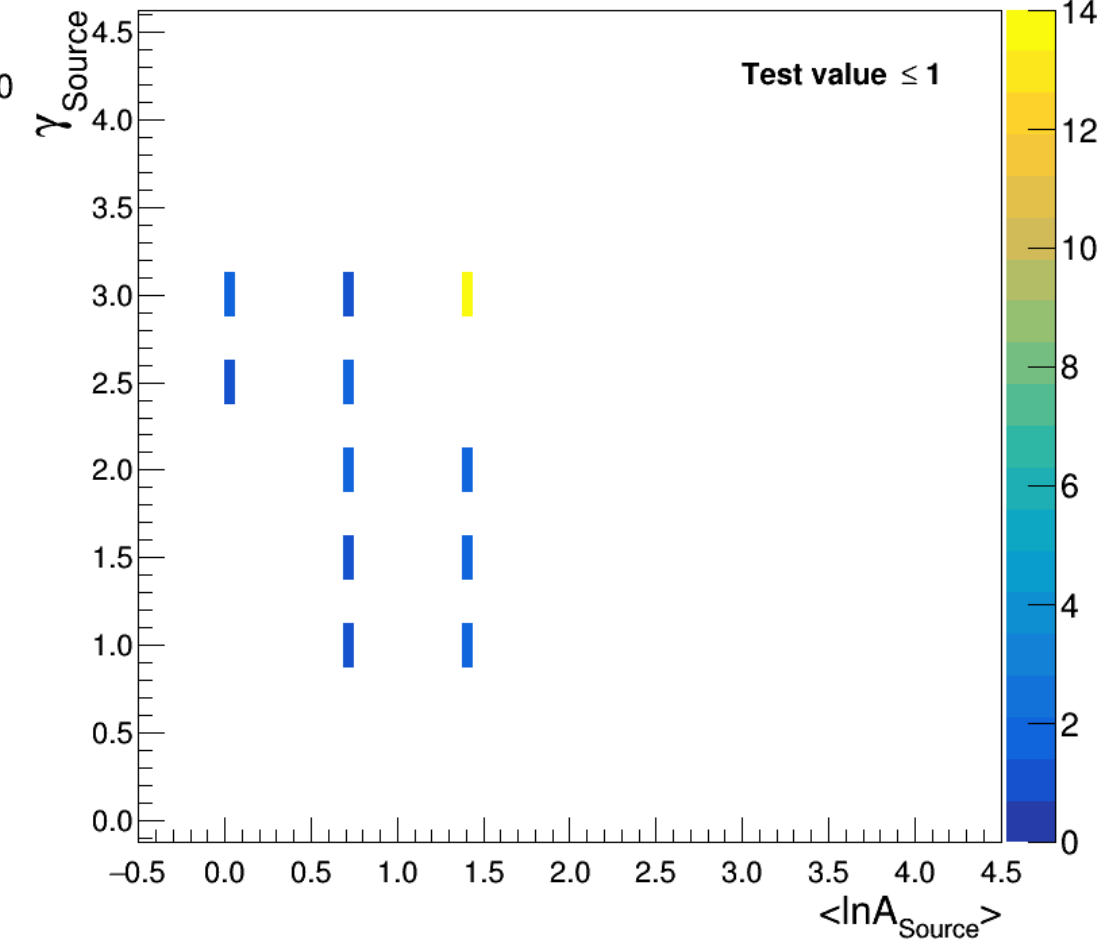


- PAO energy spectrum described by the sources with the light composition

Spectral index vs distance

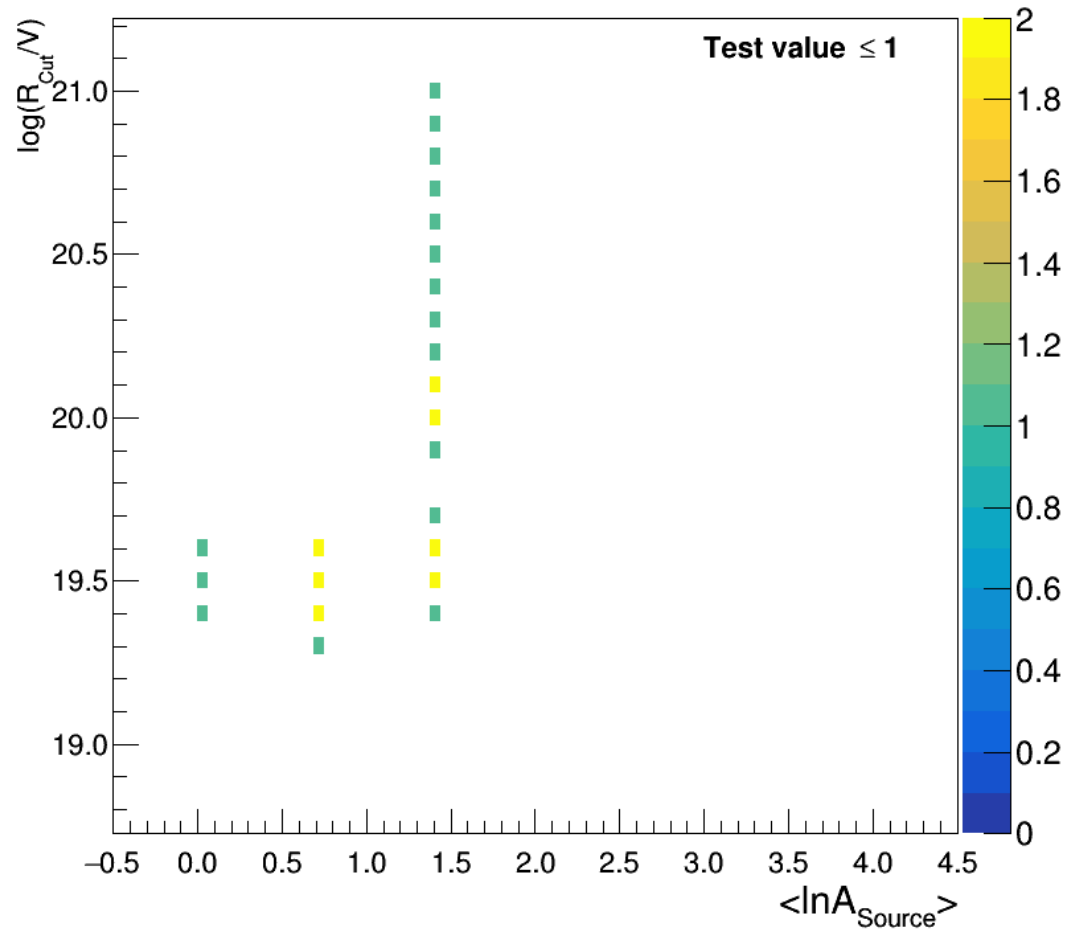


Spectral index vs primary mass composition

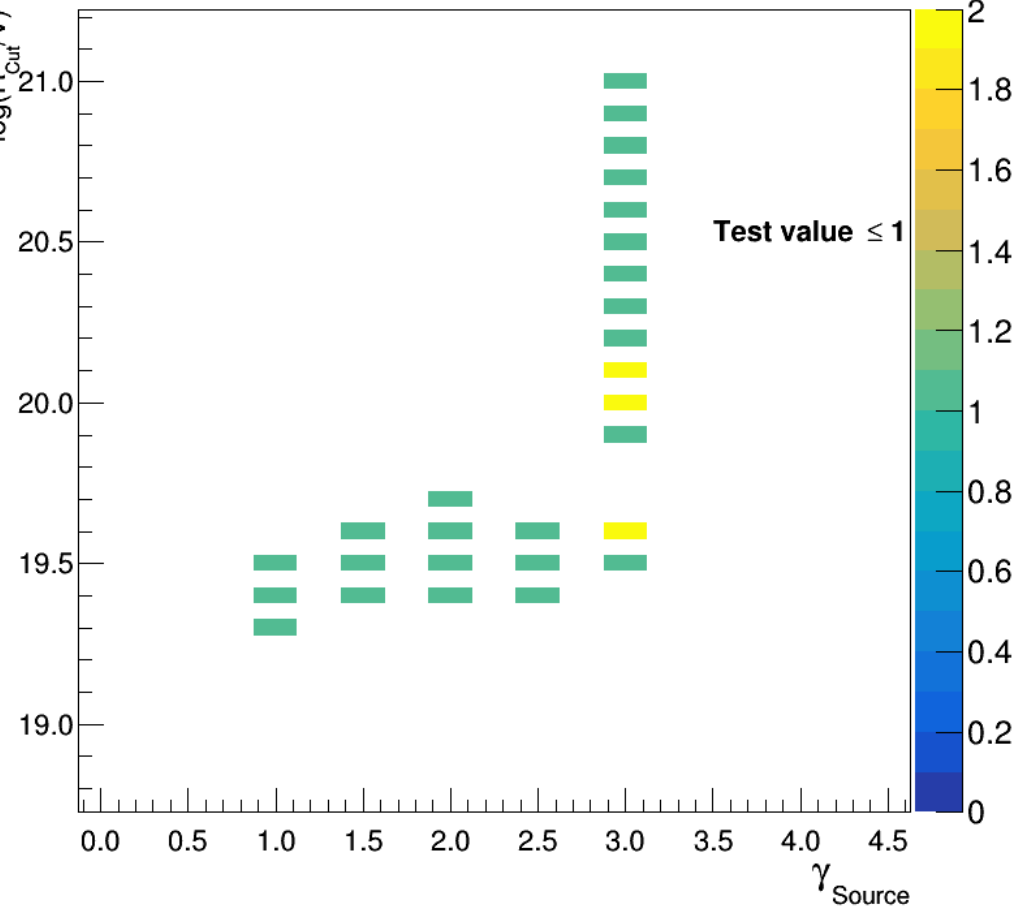


- Theoretically predicted indices are found for the closest sources

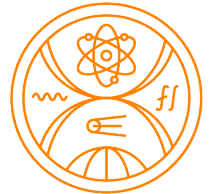
Cutoff rigidity vs primary mass composition



Cutoff rigidity vs spectral index



Summary



- Study of the evolution of $\langle \ln A_{\text{Earth}} \rangle$ - observation of the sharp increase, could be in future an indication of source features
- Study of the compatibility of the energy spectrum between measured data and simulations—sources with the light composition (similar to pure helium, pure hydrogen or the combination of both) were found to be able to describe the observed shape of the energy spectrum at the very end
- Considering spectral indices in the theoretical region 1.0 – 2.2, only sources with the rigidity cutoff of value $\approx 10^{19.5} \text{ V}$ described the shape of the measured energy spectrum well. This is about one order of magnitude higher than the results of the combined fit of mass composition and energy spectrum by the Pierre Auger Observatory.





Thank you for your attention



| reference model (SPG – EPOS-LHC) | main minimum | | 2nd minimum | |
|--|-------------------------|------------------------|--------------------|------------------------|
| | best fit | average | best fit | average |
| \mathcal{L}_0 [10^{44} erg Mpc $^{-3}$ yr $^{-1}$] | 4.99 | | 9.46* | |
| γ | $0.96^{+0.08}_{-0.13}$ | 0.93 ± 0.12 | 2.04 ± 0.01 | $2.05^{+0.02}_{-0.04}$ |
| $\log_{10}(R_{\text{cut}}/\text{V})$ | $18.68^{+0.02}_{-0.04}$ | 18.66 ± 0.04 | 19.88 ± 0.02 | 19.86 ± 0.06 |
| $f_{\text{H}}(\%)$ | 0.0 | $12.5^{+19.4}_{-12.5}$ | 0.0 | $3.3^{+5.2}_{-3.3}$ |
| $f_{\text{He}}(\%)$ | 67.3 | $58.6^{+12.6}_{-13.5}$ | 0.0 | $3.6^{+6.1}_{-3.6}$ |
| $f_{\text{N}}(\%)$ | 28.1 | $24.6^{+8.9}_{-9.1}$ | 79.8 | $72.1^{+9.3}_{-10.6}$ |
| $f_{\text{Si}}(\%)$ | 4.6 | $4.2^{+1.3}_{-1.3}$ | 20.2 | $20.9^{+4.0}_{-3.9}$ |
| $f_{\text{Fe}}(\%)$ | 0.0 | | 0.0 | |
| D/n | $174.4/119$ | | $235.7/119$ | |
| D (J), D (X_{max}) | 13.3, 161.1 | | 19.5, 216.2 | |
| p | 0.026 | | 5×10^{-4} | |

*From $E_{\text{min}} = 10^{15}$ eV.

| option | description | default |
|-----------|---|---------|
| -h | prints the help and exits | none |
| -s | seed of the random number generator | 65539 |
| -N | number of events to be generated | 100 |
| -A | mass number of primary nuclei, A_{inj} (chosen at random for each event with -A 0) | 56 |
| -e | $\log_{10}(E_{\text{min}}/\text{eV})$, where E_{min} is the minimum injection energy | 17 |
| -E | $\log_{10}(E_{\text{max}}/\text{eV})$, where E_{max} is the maximum injection energy | 21 |
| -g | injection spectral index, γ | 1 |
| -z | minimum source redshift, z_{min} | 0 |
| -Z | maximum source redshift, z_{max} | 1 |
| -r | distance between sources, L_s , in Mpc | 0 |
| -L | EBL model, see section | 1 |
| -M | photodisintegration model, see section | 0 |
| -n | nucleon ejection scaling factor (only with -M 3 and -M 4) | 1 |
| -a | alpha-particle ejection scaling factor (only with -M 3 and -M 4) | 1 |
| -D | beta decay: 0 disabled, all nuclei treated as their respective beta-decay stable isobars; 1 enabled, treated as instantaneous | 1 |

(Aloisio et al., 2017)

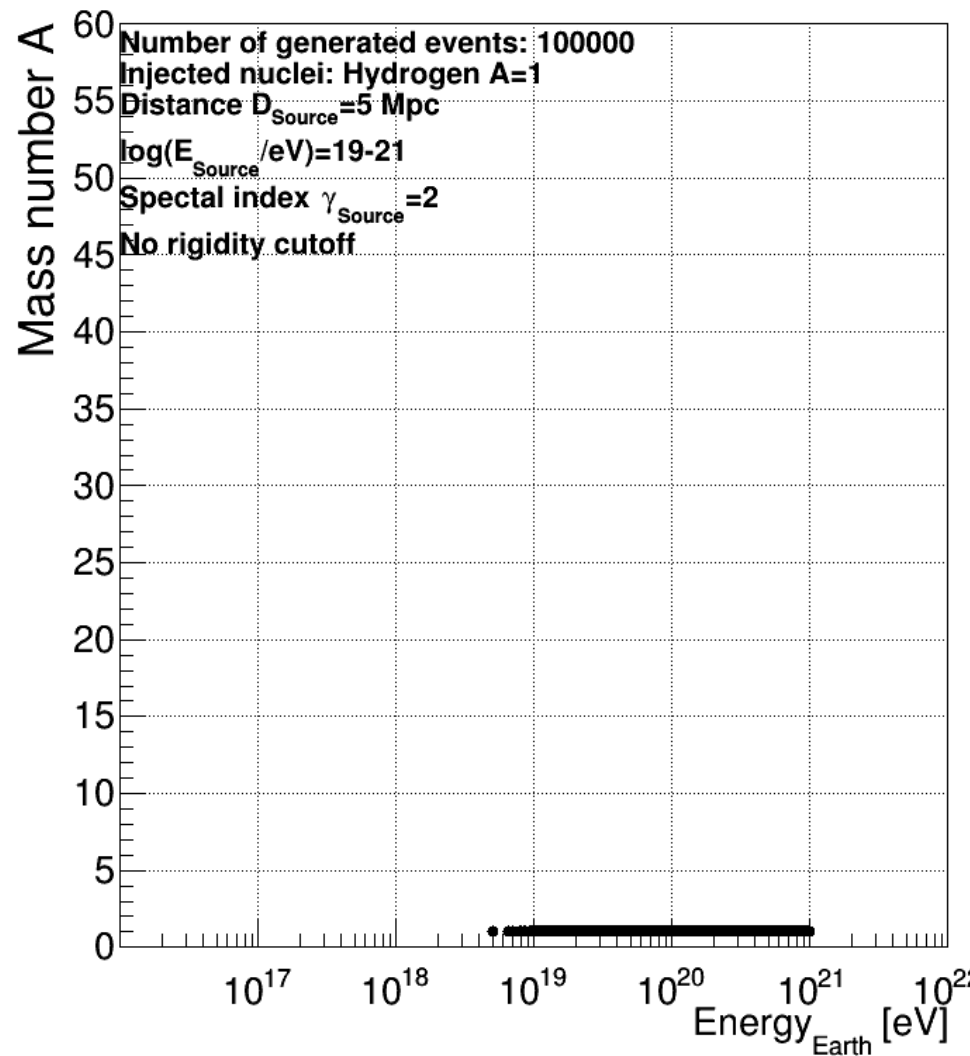
| option | description | default |
|--------|---|---------|
| -s | treatment of pion production: -1 continuous energy loss approximation for protons, neglected for other nuclei (as in <i>SimProp</i> v2r0); 0 continuous energy loss for both protons and other nuclei; 1 stochastic, on the CMB only; 2 stochastic, on both the CMB and the EBL | 1 |
| -p | electrons and positrons: 0 disregarded, 1 individually written to output file (warning: results in very large output files), 2 binned according to production redshift (by default $[10^{-4.0}, 10^{-3.8}], \dots, [10^{+0.8}, 10^{+1.0}]$), but can be changed in the file <code>src/Output.h</code> before compiling), 3 only total energy written | 0 |
| -o | output type (see below): 0 old (<code>nuc</code> and <code>ev</code> trees); 1 new (<code>summary</code> tree); 2 both | 0 |

(Aloisio et al., 2017)

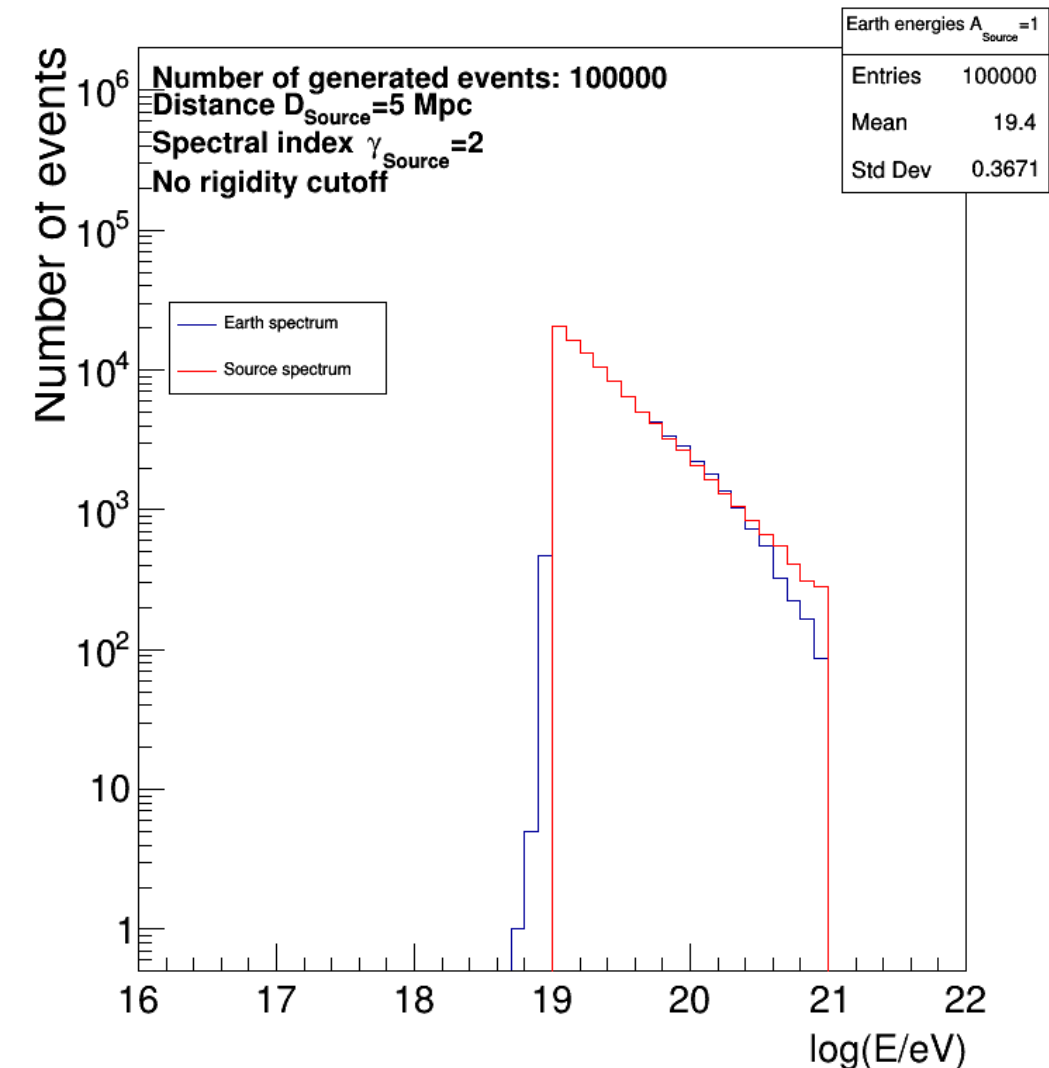
Analysis for close sources

Hydrogen

Mass spectrum

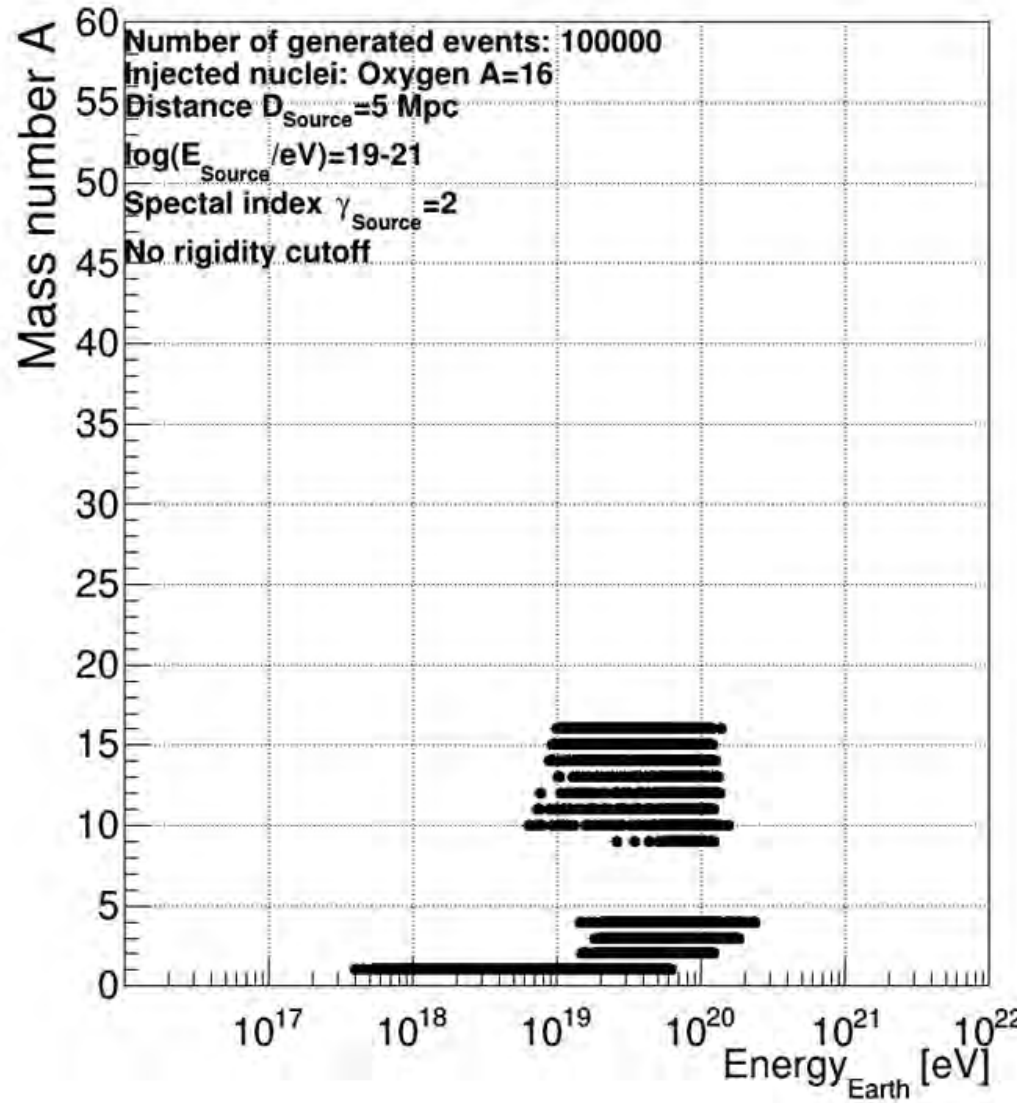


Energy spectrum

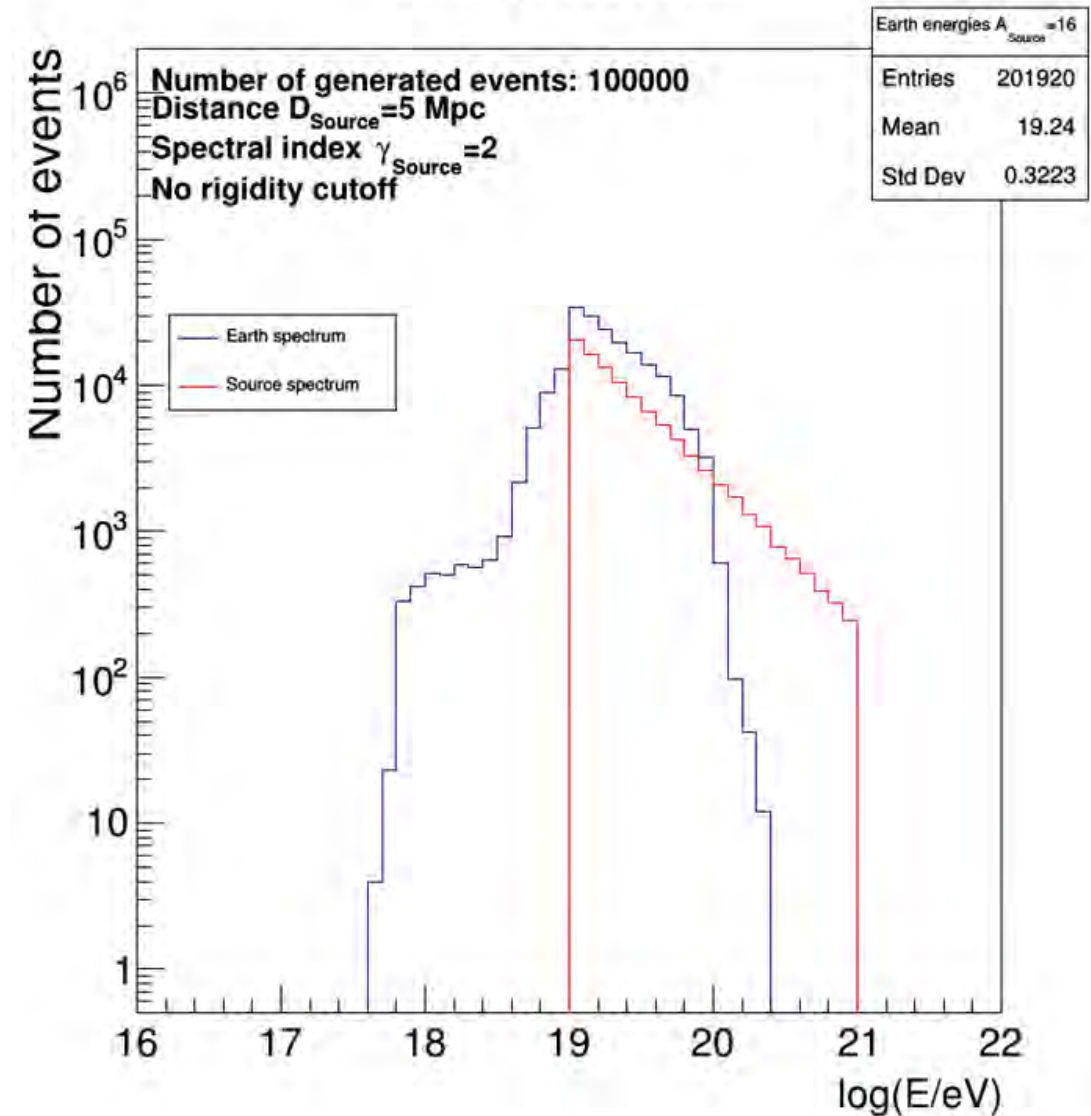


Oxygen

Mass spectrum

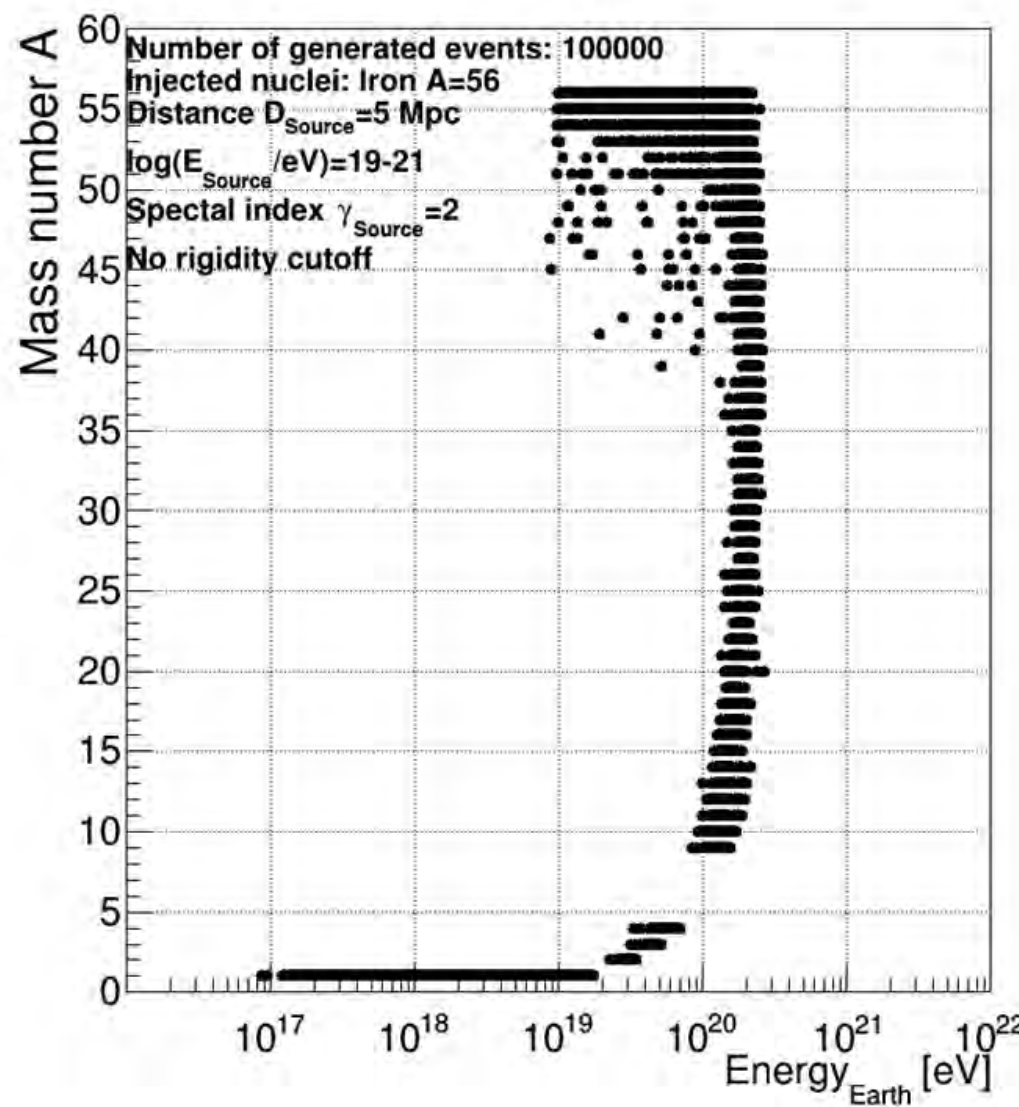


Energy spectrum

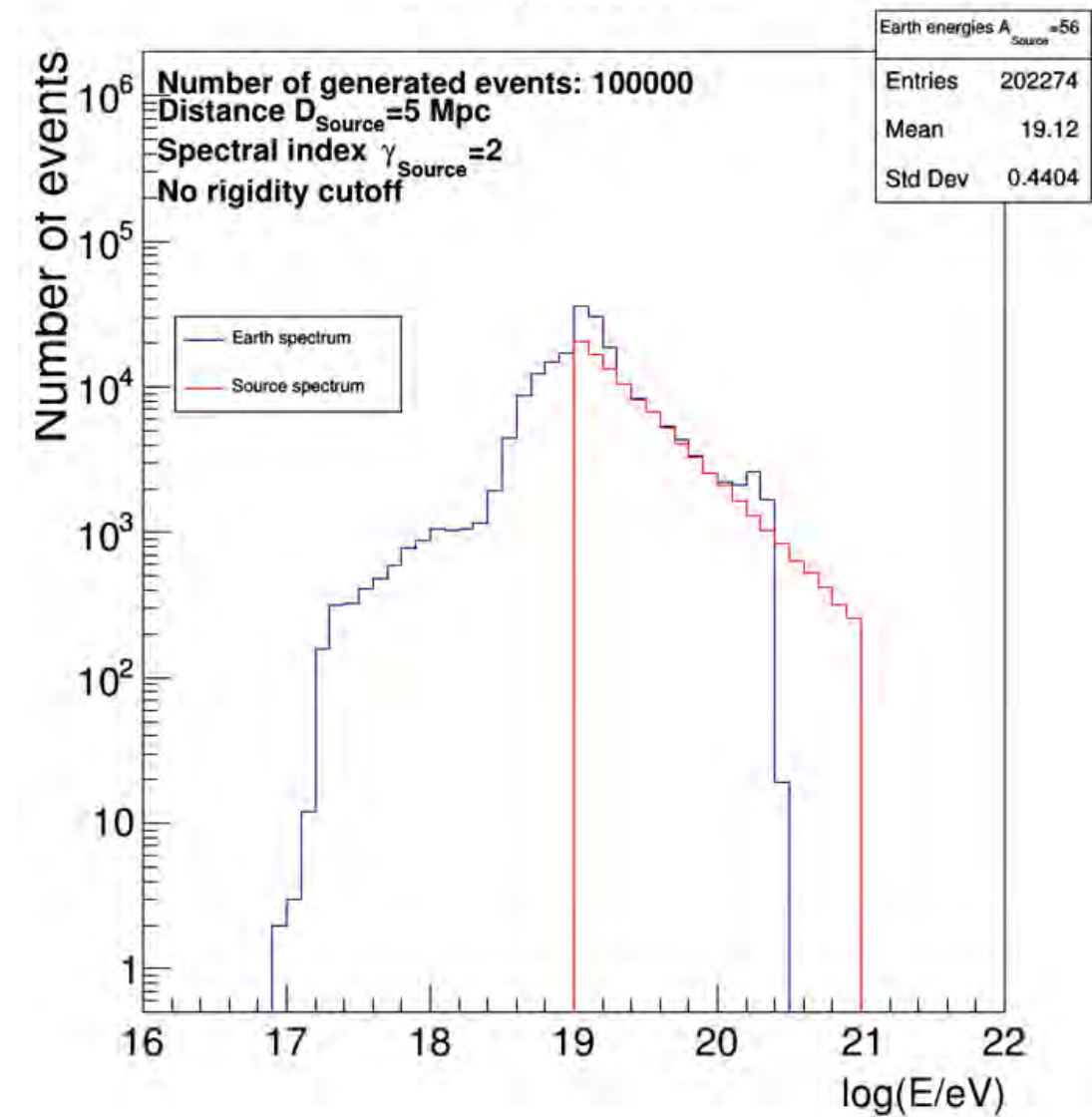


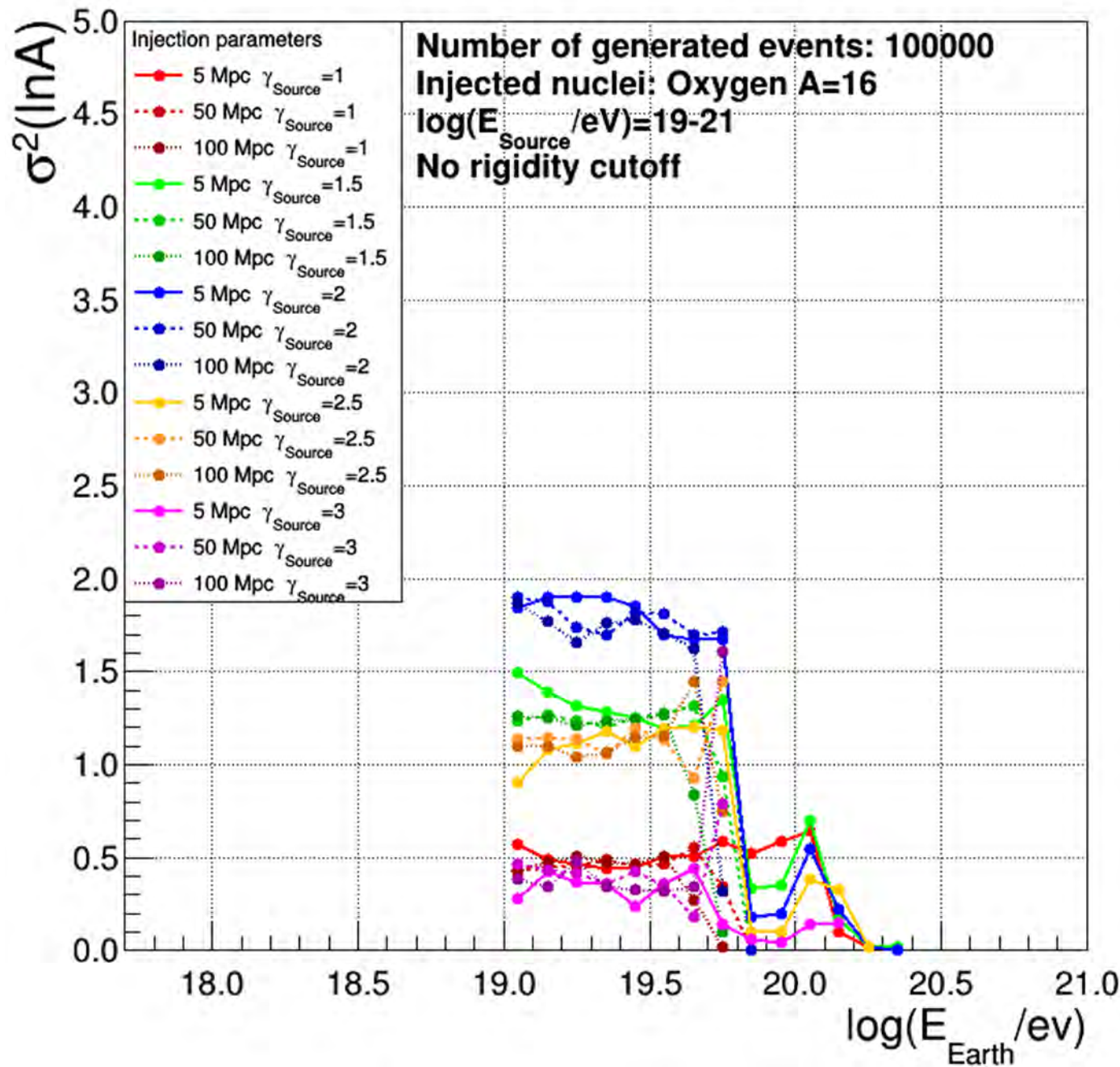
Iron

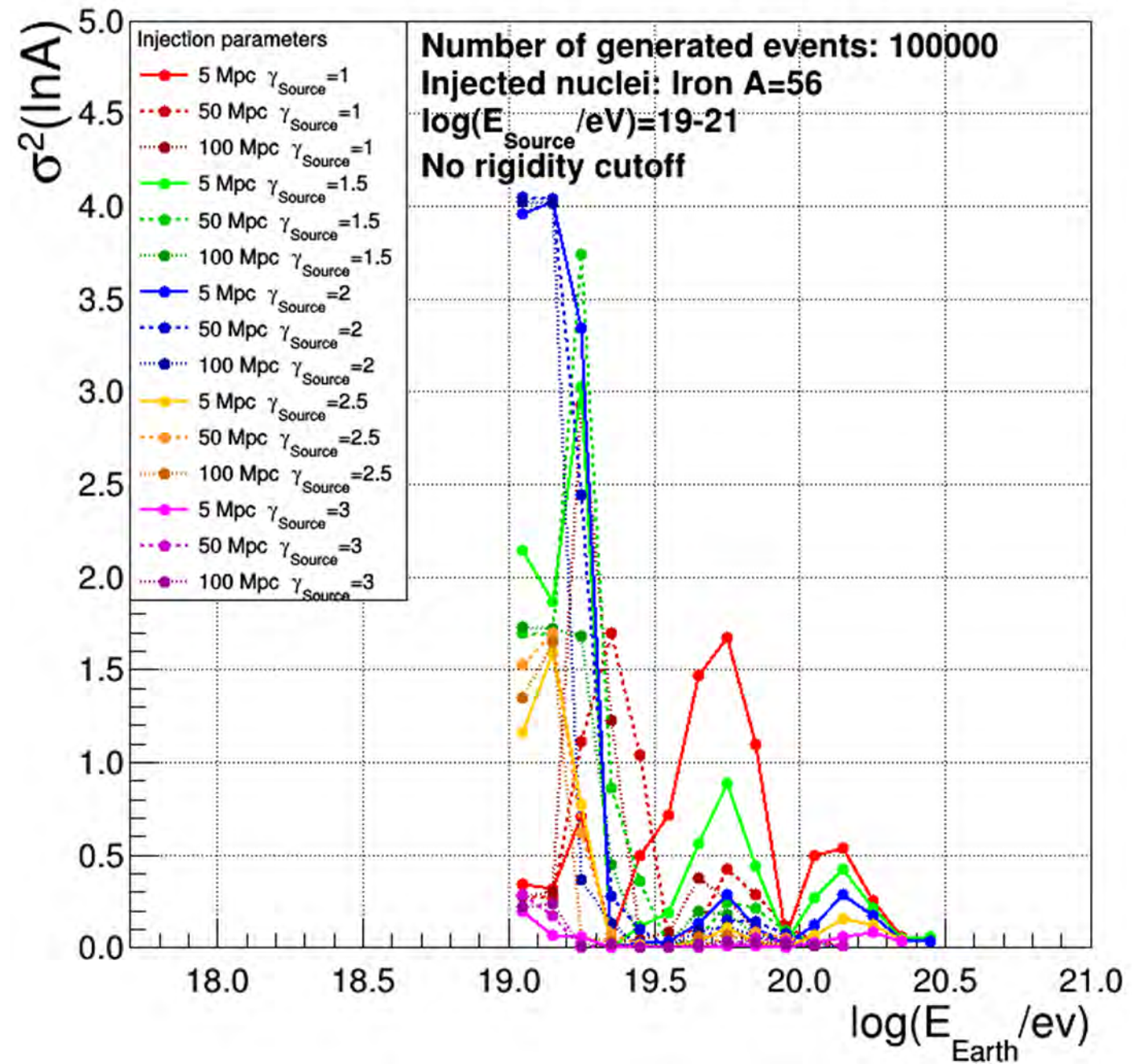
Mass spectrum

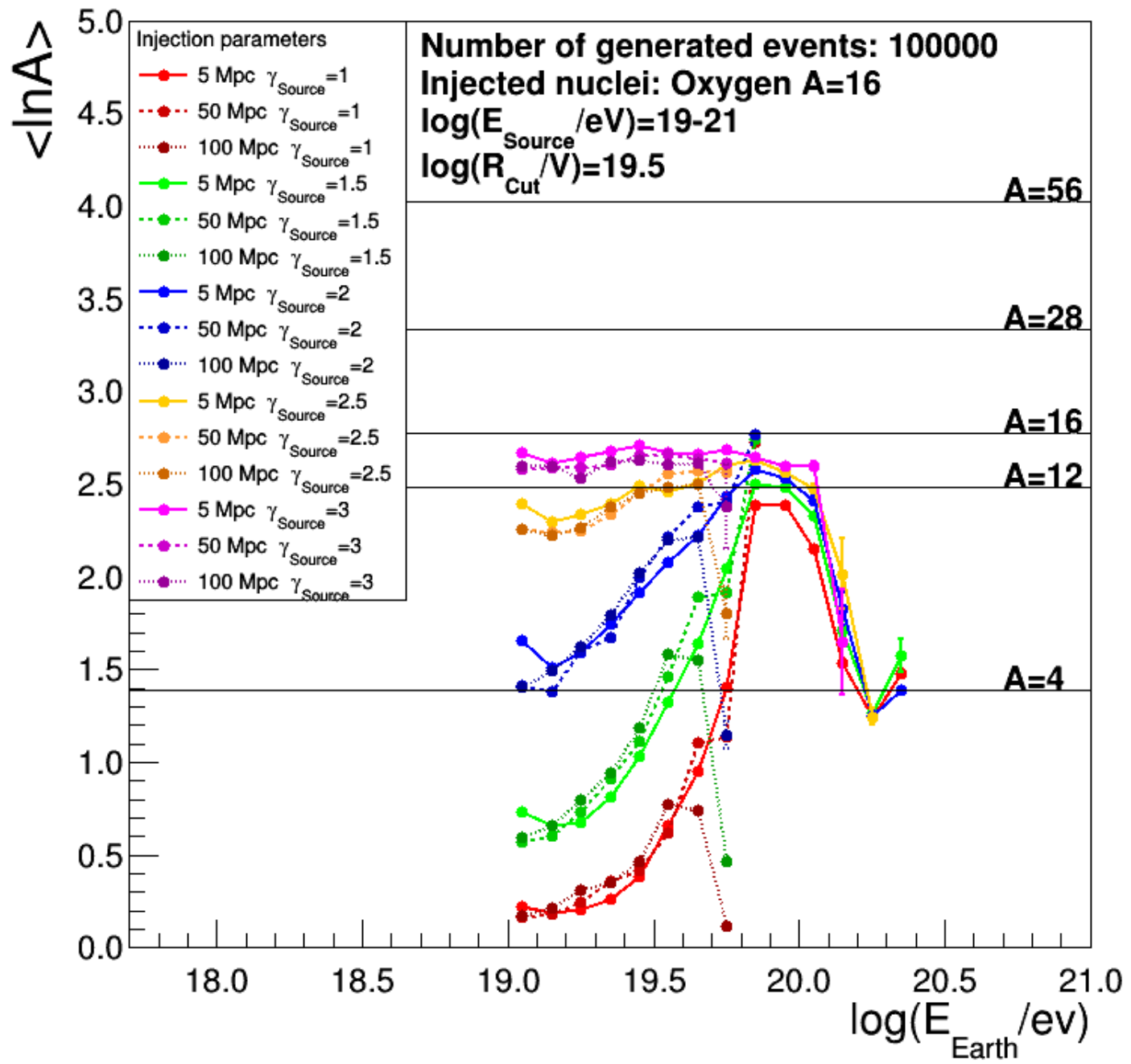


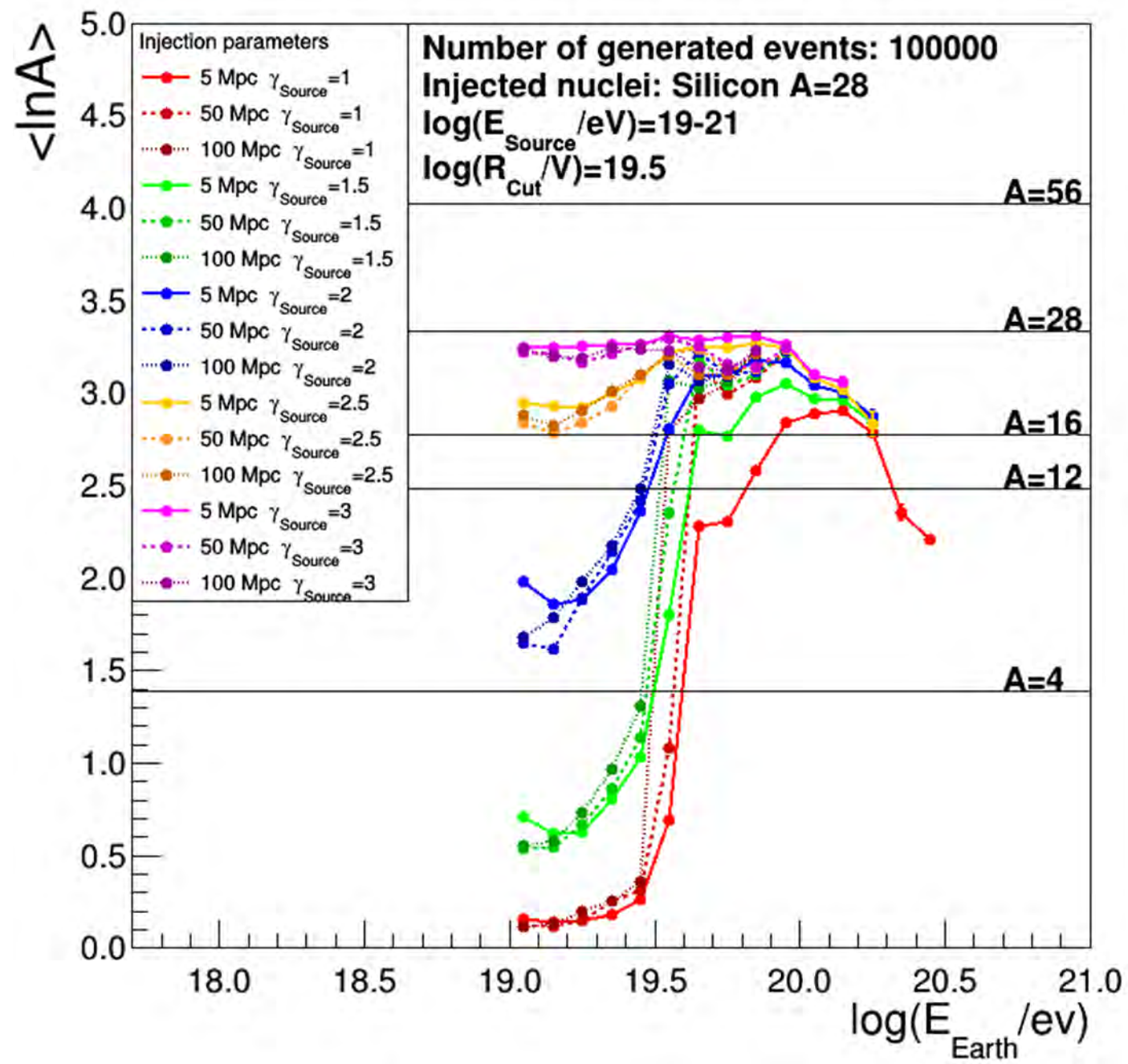
Energy spectrum

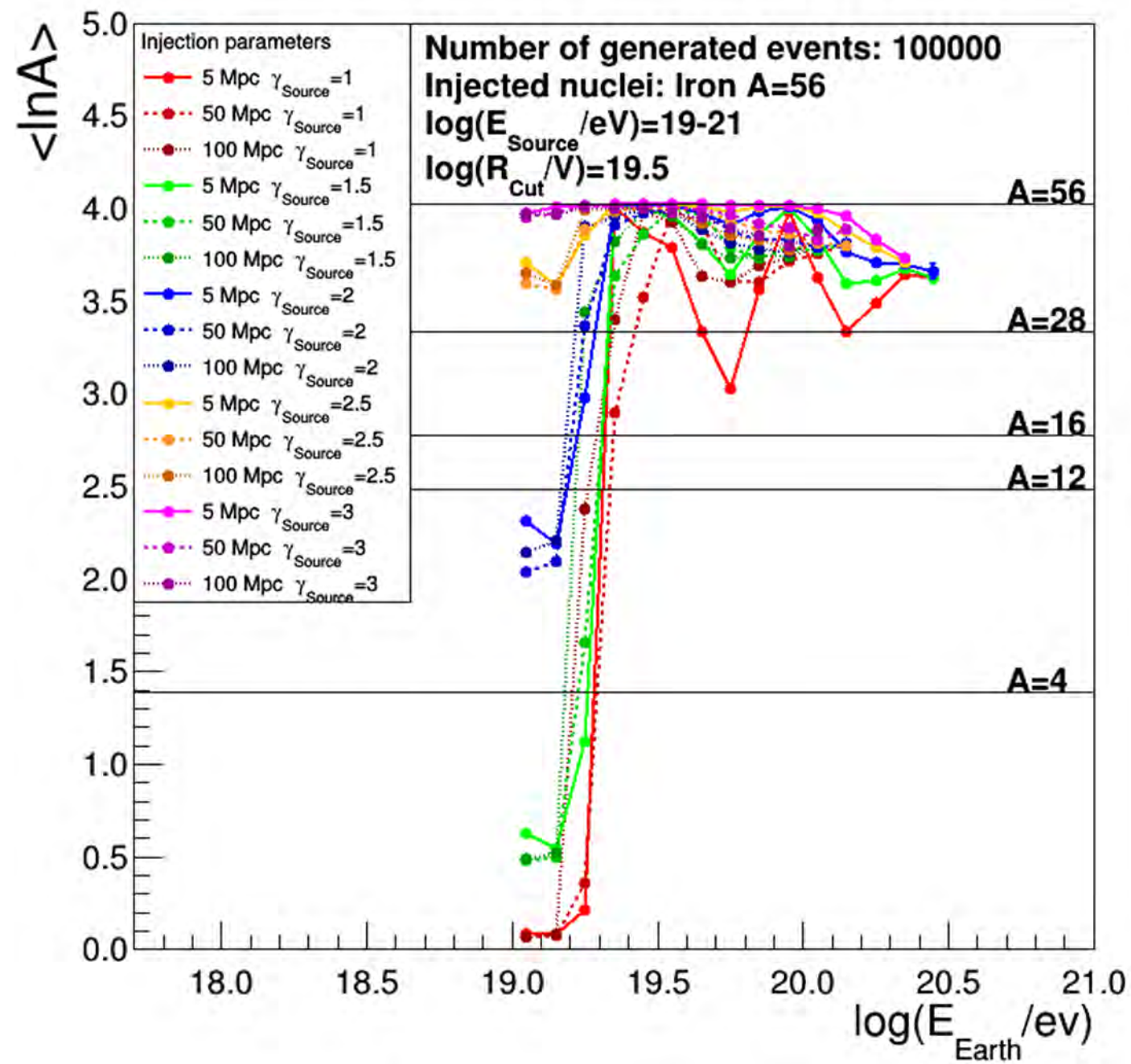




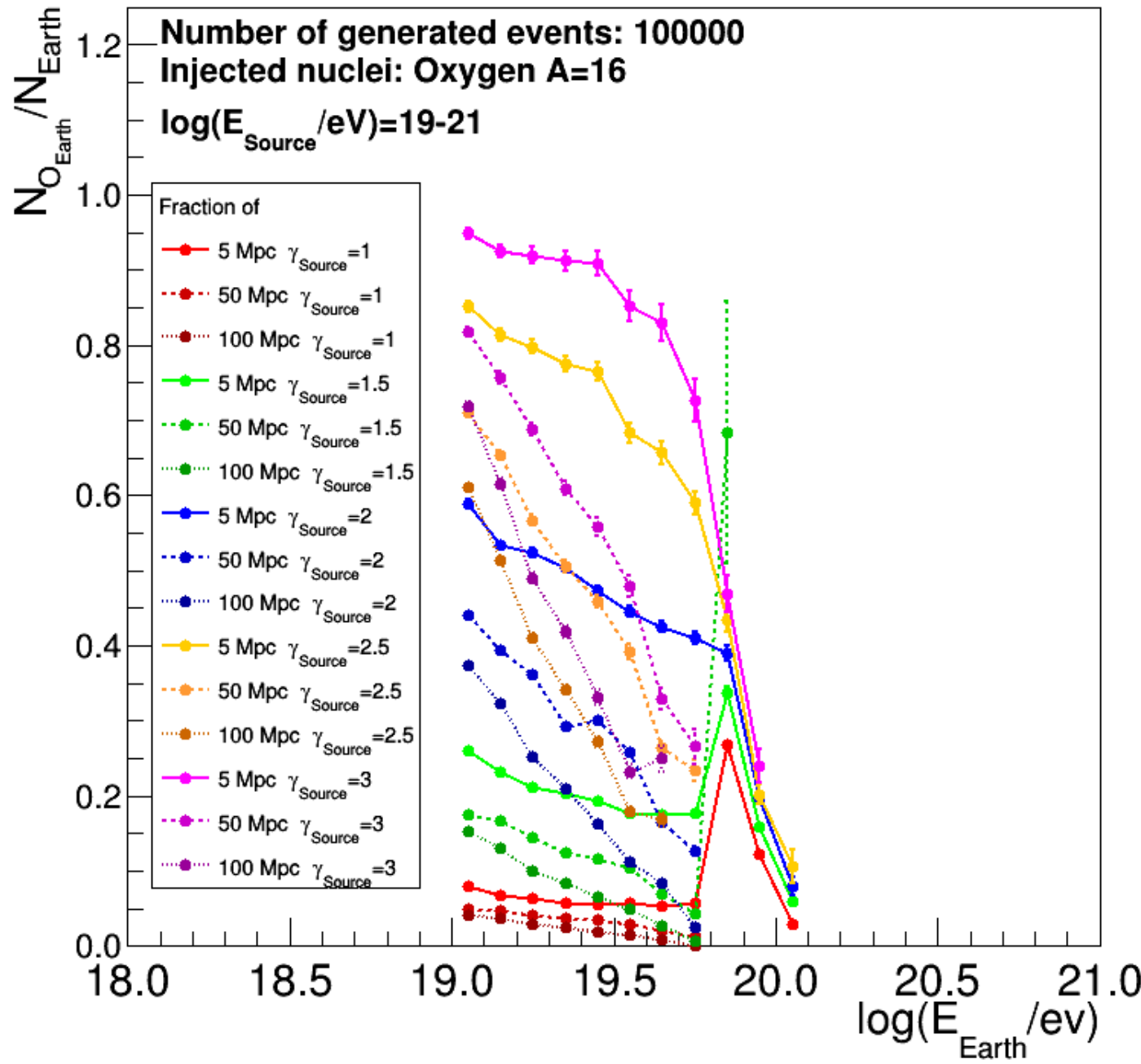




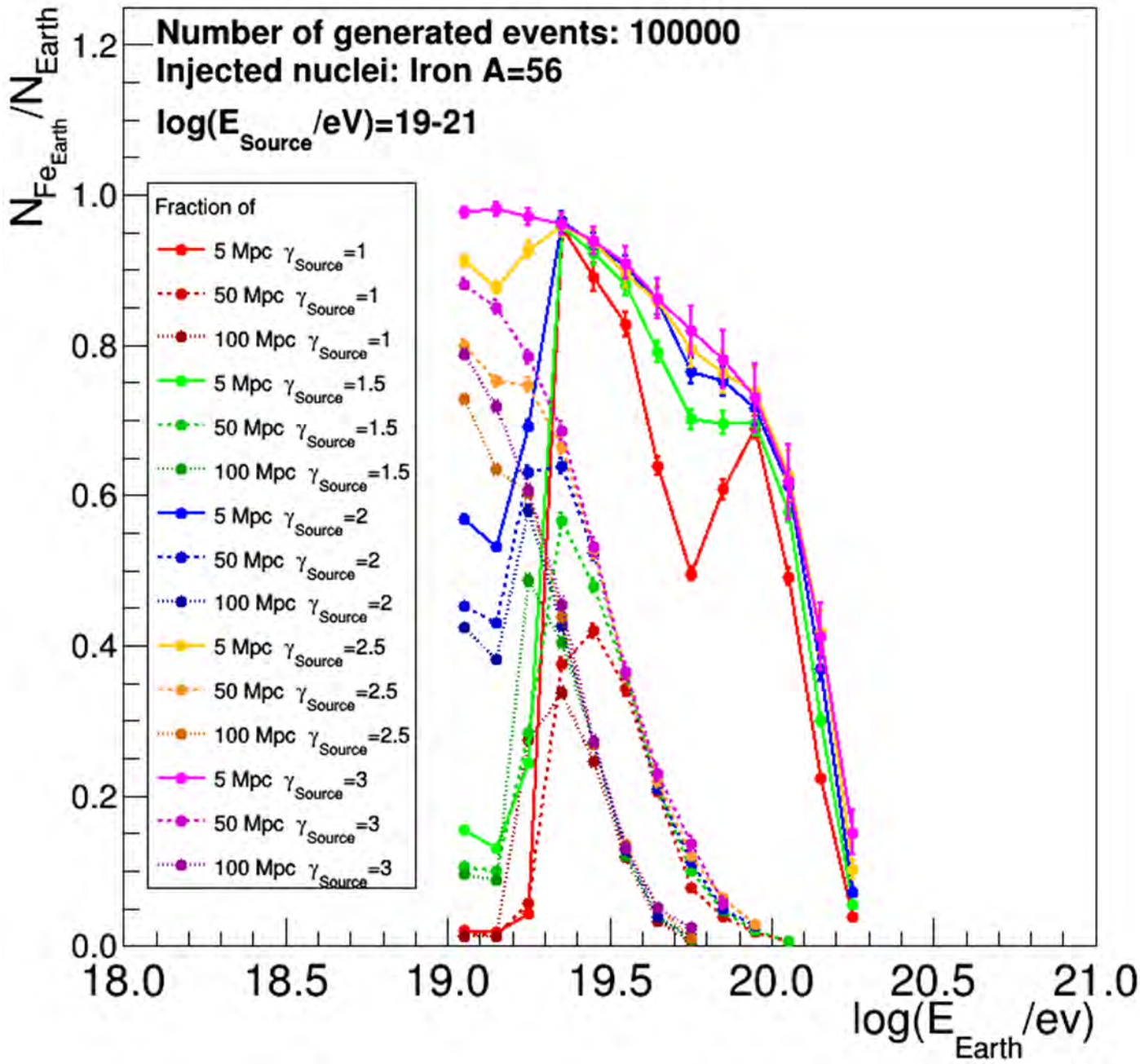




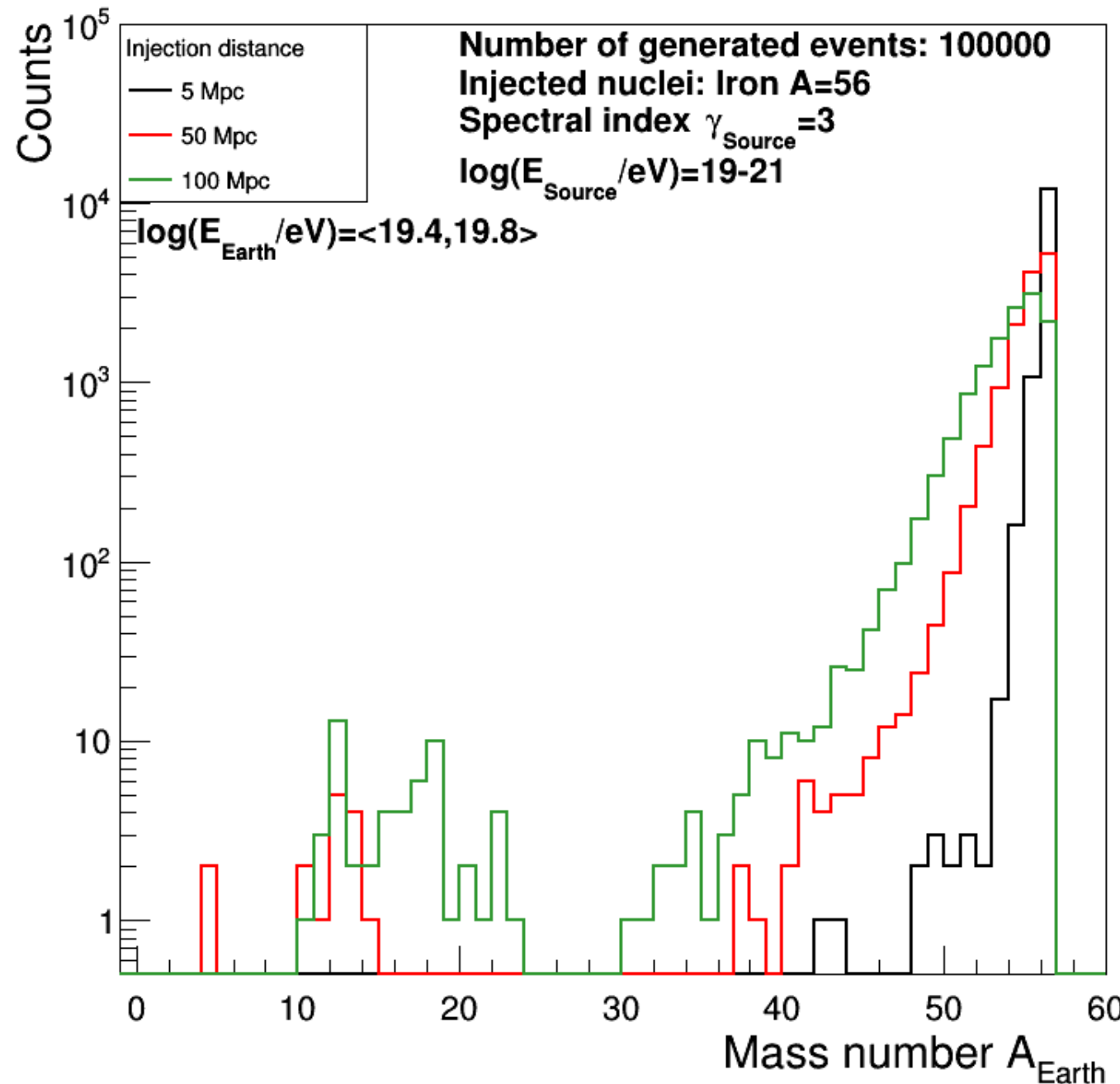
Fraction of oxygen nuclei on Earth



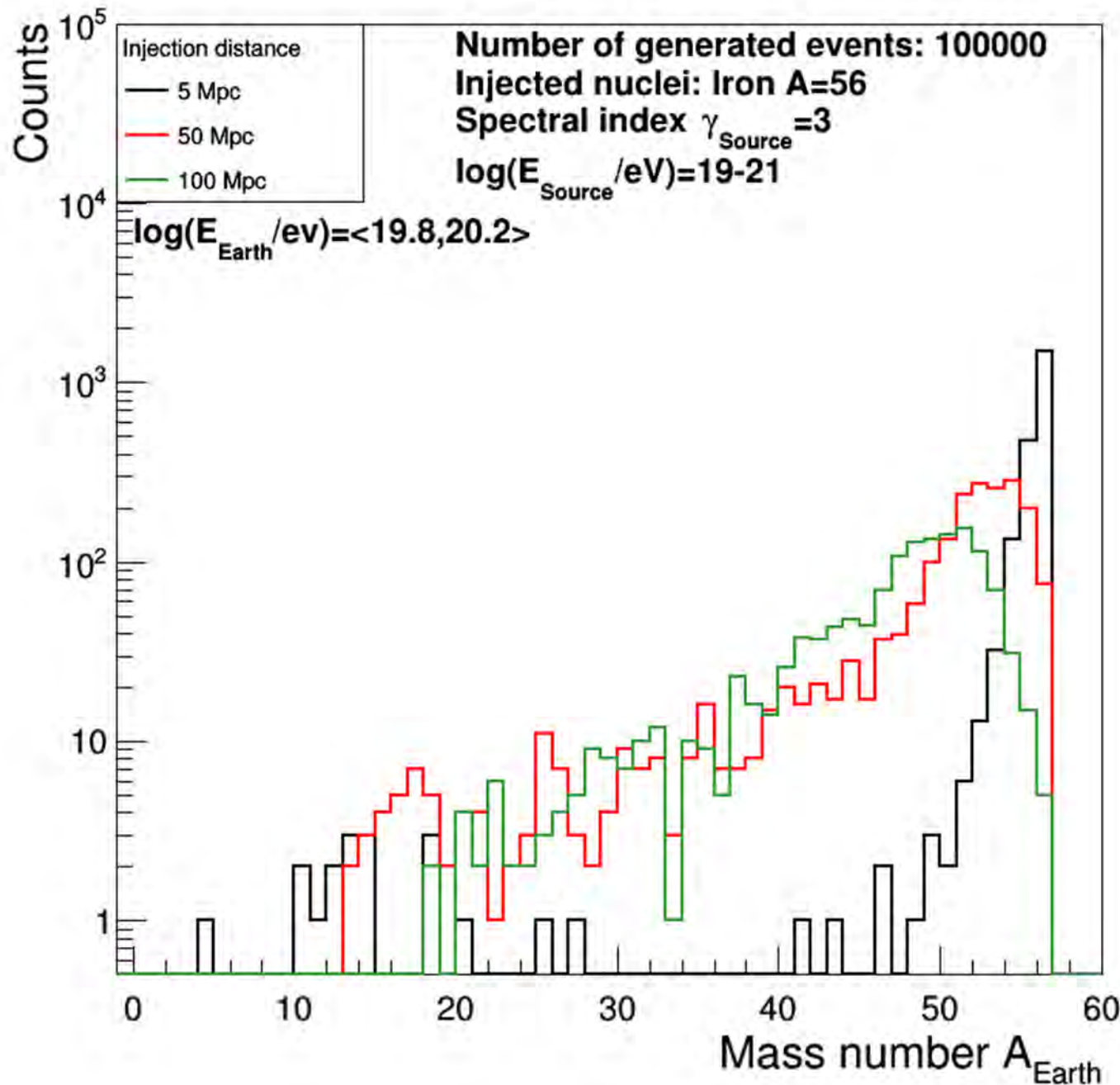
Fraction of iron nuclei on Earth



Distribution of mass number A



Distribution of mass number A



| Combination | $\langle \ln A_{\text{Source}} \rangle$ |
|-------------|---|
| H | 0 |
| He | 1.386 |
| O | 2.773 |
| Fe | 4.025 |
| H+He | 0.693 |
| H+O | 1.386 |
| H+Fe | 2.013 |
| He+O | 2.079 |
| He+Fe | 2.706 |
| O+Fe | 3.399 |
| H+He+O | 1.386 |
| H+He+Fe | 1.804 |
| H+O+Fe | 2.266 |
| He+O+Fe | 2.728 |
| H+He+O+Fe | 2.046 |

